International Journal of Photoenergy

Advances in Design and Application of Photovoltaic/ Thermal Systems

Lead Guest Editor: Muhammad Imtiaz Hussain
Guest Editors: Kamaruzzaman Sopian and Amin Shahsavar

Advances in Design and Application of Photovoltaic/Thermal Systems

International Journal of Photoenergy

Advances in Design and Application of Photovoltaic/Thermal Systems

Lead Guest Editor: Muhammad Imtiaz Hussain
Guest Editors: Kamaruzzaman Sopian and Amin Shahsavar

Copyright © 2022 Hindawi Limited. All rights reserved.

This is a special issue published in “International Journal of Photoenergy.” All articles are open access articles distributed under the Creative Commons Attribution License, which permits unrestricted use, distribution, and reproduction in any medium, provided the original work is properly cited.

Chief Editor

Giulia Grancini, Italy

Academic Editors

Mohamed S.A. Abdel-Mottaleb, Egypt
Angelo Albini, Italy
Mohammad Alghoul, Malaysia
Alberto Álvarez-Gallegos, Mexico
Vincenzo Augugliaro, Italy
Detlef W. Bahnemann, Germany
Simona Binetti, Italy
Fabio Bisegna, Italy
Thomas M. Brown, Italy
Joaquim Carneiro, Portugal
Yatendra S. Chaudhary, India
Kok-Keong Chong, Malaysia
Věra Cimrová, Czech Republic
Laura Clarizia, Italy
Gianluca Coccia, Italy
Daniel Tudor Cotfas, Romania
P. Davide Cozzoli, Italy
Dionysios D. Dionysiou, USA
Elisa Isabel Garcia-Lopez, Italy
Wing-Kei Ho, Hong Kong
Siamak Hoseinzadeh, Italy
Jürgen Hüpkes, Germany
Fayaz Hussain, Brunei Darussalam
Mohamed Gamal Hussien, Egypt
Adel A. Ismail, Kuwait
Chun-Sheng Jiang, USA
Zaiyong Jiang, China
Yuanzuo Li, China
Manuel Ignacio Maldonado, Spain
Santolo Meo, Italy
Claudio Minero, Italy
Regina De Fátima Peralta Muniz Moreira, Brazil
Maria da Graça P. Neves, Portugal
Tsuyoshi Ochiai, Japan
Kei Ohkubo, Japan
Umapada Pal, Mexico
Dillip K. Panda, USA
Carlo Renno, Italy
Francesco Riganti-Fulginei, Italy
Leonardo Sandrolini, Italy
Jinn Kong Sheu, Taiwan
Kishore Sridharan, India
Elias Stathatos, Greece
Jegadesan Subbiah, Australia
Chaofan Sun, China
K. R. Justin Thomas, India
Koray Ulgen, Turkey
Ahmad Umar, Saudi Arabia
Qiliang Wang, China
Xuxu Wang, China
Huiqing Wen, China
Weijie Yang, China
Jiangbo Yu, USA

Contents

Hindawi
International Journal of Photoenergy
Volume 2022, Article ID 3186378, 18 pages
https://doi.org/10.1155/2022/3186378

Research Article

Machine Learning-Based Relative Performance Analysis of Monocrystalline and Polycrystalline Grid-Tied PV Systems

Asfand Yar[1], **Muhammad Yousaf Arshad**[2,3], **Faran Asghar**[4], **Waseem Amjad**[1], **Furqan Asghar**[1], **Muhammad Imtiaz Hussain**[5], **Gwi Hyun Lee**[6], **and Faisal Mahmood**[1]

[1]*Department of Energy Systems Engineering, University of Agriculture, Faisalabad, Pakistan*
[2]*Sitara Chemical Industries Pvt. Ltd., Faisalabad, Pakistan*
[3]*Department of Chemical Engineering, University of Engineering and Technology (U.E.T) Lahore, Pakistan*
[4]*School of Information Management, Nanjing University, Nanjing, China*
[5]*Agriculture and Life Sciences Research Institute Kangwon National University, Chuncheon 24341, Republic of Korea*
[6]*Interdisciplinary Program in Smart Agriculture, Kangwon National University, Chuncheon 24341, Republic of Korea*

Correspondence should be addressed to Gwi Hyun Lee; ghlee@kangwon.ac.kr and Faisal Mahmood; faisal.mahmood@uaf.edu.pk

Received 1 March 2022; Revised 17 June 2022; Accepted 11 July 2022; Published 12 August 2022

Academic Editor: Alberto Álvarez-Gallegos

Copyright © 2022 Asfand Yar et al. This is an open access article distributed under the Creative Commons Attribution License, which permits unrestricted use, distribution, and reproduction in any medium, provided the original work is properly cited.

In this research study, the design and performance evaluation of grid-tied photovoltaic systems has been carried out through experimentation, HelioScope simulation, and black-box machine learning methods for data-driven artificial intelligence system performance assessment and validation. The proposed systems are based on 15 kWp of monoperk and polyperk, which are separately installed in the industrial sector of Faisalabad, Pakistan. The experimental evaluation of the installed PV modules was performed from November 2020 to August 2021. The performance of the PV modules was evaluated by determining the annual average daily final yield (If), performance ratio (PR), and capacity factor (CF). The study showed that the annual average of daily final yield, performance ratio, and capacity factor for 15 kW polyperk was estimated to be 61.94 kWh, 84.17%, and 19.12, respectively. The annual average of daily final yield, performance ratio, and capacity factor for 15 kW monoperk was estimated to be 58.32 kWh, 81.42%, and 18.13, respectively. A comparison of final yield is obtained from simulation and real-time systems obtained from polyperk PV and monoperk. A significant mean error exists between the experimentation and simulation results which lie within the range of 1250 to 1470 kWh and 1600 to 1950 kWh, respectively. Substantial differences between both aforementioned results were initially tested and highlighted by statistical values; i.e., the standard error lies in-between 5 and 45% in polyperk crystalline and 5 and 25% in monocrystalline PV grid-connected module. Machine learning logistical regression evaluated that monoperk crystalline grid-connected system, experimental work was found to be more reliable with error difference reduces in off-peak months as compared to corresponding simulation study and vice versa for polyperk crystalline grid-connected system. Model accuracy after training and testing produced resulted up to 99.5% accuracy for either grid-connected experimentation or simulation outcomes with validation.

1. Introduction

In any country, energy is one of the key factors for the smooth and faster upgradation of the socioeconomic activities, and it has become a universal fact now. One of the major drivers of economic growth is energy as identified by the government of Pakistan. Therefore, Pakistan requires adequate supplies of energy for the generation of healthy economic activities. The country currently is passing through the worst energy crisis in over 70 years. The energy crisis has led to the hindrance of socioeconomic progress below the level of critical sustainability and tolerance of the people. Pakistan has a land area of 881,913 km^2 consisting of a population of 211.117 million [1]. In 2019, Pakistan's electricity

generation was recorded to be 87.3 TWh [1]. The energy mix of Pakistan's energy scenario depicts that thermal energy is the widest energy resource upon which Pakistan has been relying in recent years. To warrant adequate, secure, and cheap energy supply to industries, transportation, domestic needs, and agriculture availing available resources in such a manner that it minimizes its losses should be the main objectives of the energy sector. For the proper growth of renewable energy sectors, they must be given the chance in the present energy mix.

A photovoltaic system is not a new phenomenon as a plethora of literature is available on the topic. It has been in practice for the past few decades in our everyday life producing renewable energy, which is not only efficient, but it is carbon emission-free which is beneficial for the environment. Today, our technology has shifted to renewable resources, such as biomass, wind, and solar. In the development of countries, renewable energy plays a contentious role. Nowadays, the resource in trend is solar power. There are various kinds of photovoltaic (PV) power plants that can be integrated with existing power systems. PV energy plants generally use various types of PV engineering such as monocrystalline, polycrystalline, and amorphous silicon. They come as thin-film PV panels using copper indium di-selenide, copper indium gallium selenide, and cadmium telluride.

Various studies have evaluated the performance parameters of installed PV power plants in different locations, with the varying climatic condition, such as Europe [2–5], tropical regions [6, 7], Malaysia [8, 9], Oman [10], and Asian countries, India, Korea [11–15], and China [16–22]. It was observed that the performance analysis is affected by system losses, module quality, inverters, shading effect, losses in wiring, array tilt angle, and type of grid connections. The effect of these factors was confirmed by literature where a 190 kWp grid-connected PV power plant in India was evaluated [16]. In another study, it was found that these factors played a crucial role in reducing the annual average daily final yield. The efficiency of the PV module, inverter, and system was found to be 14.9%, 89.2%, and 12.6%, respectively. The capacity factor and performance ratio were found to be 10.1% and 81.5%, respectively [2]. The impact of dust is one of the significant factors which reduces the efficiency of PV modules. As compared to previously mentioned factors, the effect of dust is inferior to the performance of the PV systems [20]. Research about the performance evaluation of PV systems installed in Serbia was carried out to investigate the effects of ambient temperature and compare it with similar studies around the world. The study reports an analysis of 2 kW monocrystalline silicon (mc-Si) PV power plant tied to the grid, which was built on the rooftop in Niš, Republic of Serbia. The values of PR and CF of the reported PV power plants were articulated to be 93.6% and 12.88%, respectively [23]. Performance evaluation of polycrystalline silicon- (p-Si-) based PV systems was carried out at various locations, namely, Singapore, Turkey, and Greece, with installed capacities of 142.5 kWp, 2.73 kWp, and 171.36 kWp, respectively. From these studies, it can be observed that local varying parameters such as CF, PR, and final yield affect the performance of PV systems. PV systems have also been installed to meet the energy demands of local office buildings in Singapore. The first zero-energy office building used a 142.5 kWp p-Si grid-connected system to meet its energy demands by using inverter factors such as efficiency and losses of heat. The first performance evaluation of the PV system was carried out over 18 months, which showed a good overall PR of 81% [24]. A similar study was published where performance analysis of a 2.73 kWp mc-Si PV power station located in the Muglia climatic conditions in Turkey was performed wherein winter thy efficiency of mono PV module is increased. According to a study carried out in Greece, a performance analysis of a fully monitored 171.36 kWp p-Si grid-connected PV system was done on an hourly, daily, and monthly basis [4].

The claim regarding the change in the tilt angle of PV modules and the change in efficiency can be supported by a report coming from Italy. This article focused on the influence of climatic conditions on a 960 kWp mc-Si-based PV power plant. The installed systems were divided into two subfields with varying tilt angles and nominal powers (i.e., 606.6 kWp and 353.3 kWp). The results revealed that the performance ratio varied between 79% and 86.5% from March to October 2012 [24]. Another study from Italy (northern), articulated the functioning of two grid-tied PV systems (i.e., 17.94 kWp and 15.9 kWp) with the same factories but possessing varying PV technology, their rated power, and overall efficiency. The performance ratio was observed, over a year, to be 89.1% for the first mc-Si wafer-based PV system and 82.7% for the second mc-Si-based PV system [25].

Although PV systems have been around for quite some time but there is no articulated study from this region that evaluates the performance of installed systems according to the region's environmental conditions, to the best of our knowledge, there has not been a study conducted that takes advantage of machine learning algorithms for the difference in performance evaluation between installed and simulated PV systems. This study has been carried out to evaluate the performance of installed PV systems located in the outskirts of Faisalabad on the same rooftop of an industry. The objectives of this study were to investigate the difference between power obtained from installed PV systems and via simulation software. Further, a machine learning algorithm was applied to analyze the performance of installed systems for cost and timesaving in the future. The PV systems (15 kWp) have been analyzed over a time of seven months. The renewable systems were based on polyperk and monoperk types of PV modules. Moreover, to classify hyperparameter results of categorical division between experimental and simulation results, machine learning-based logistical regression has been introduced. Machine learning algorithm contains the error to a minimum and provides useful insight, corelation, and evaluation with class distinction according to subjective weather and time horizon.

2. Designing of Solar Photovoltaic System

The PV systems are located at a latitude of 31.47° N, a longitude of 73.22° E, and an altitude of 186 m above sea level in the outskirts of Faisalabad city in Pakistan (Figure 1).

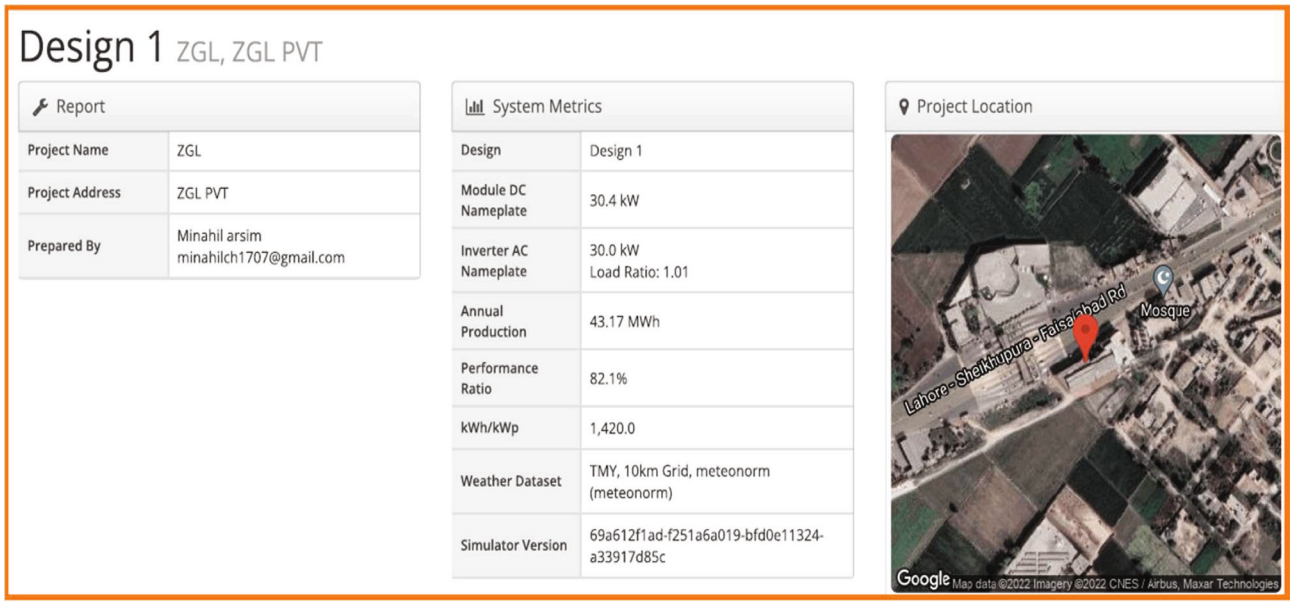

Figure 1: Simulation of installed PV system (15 kWp).

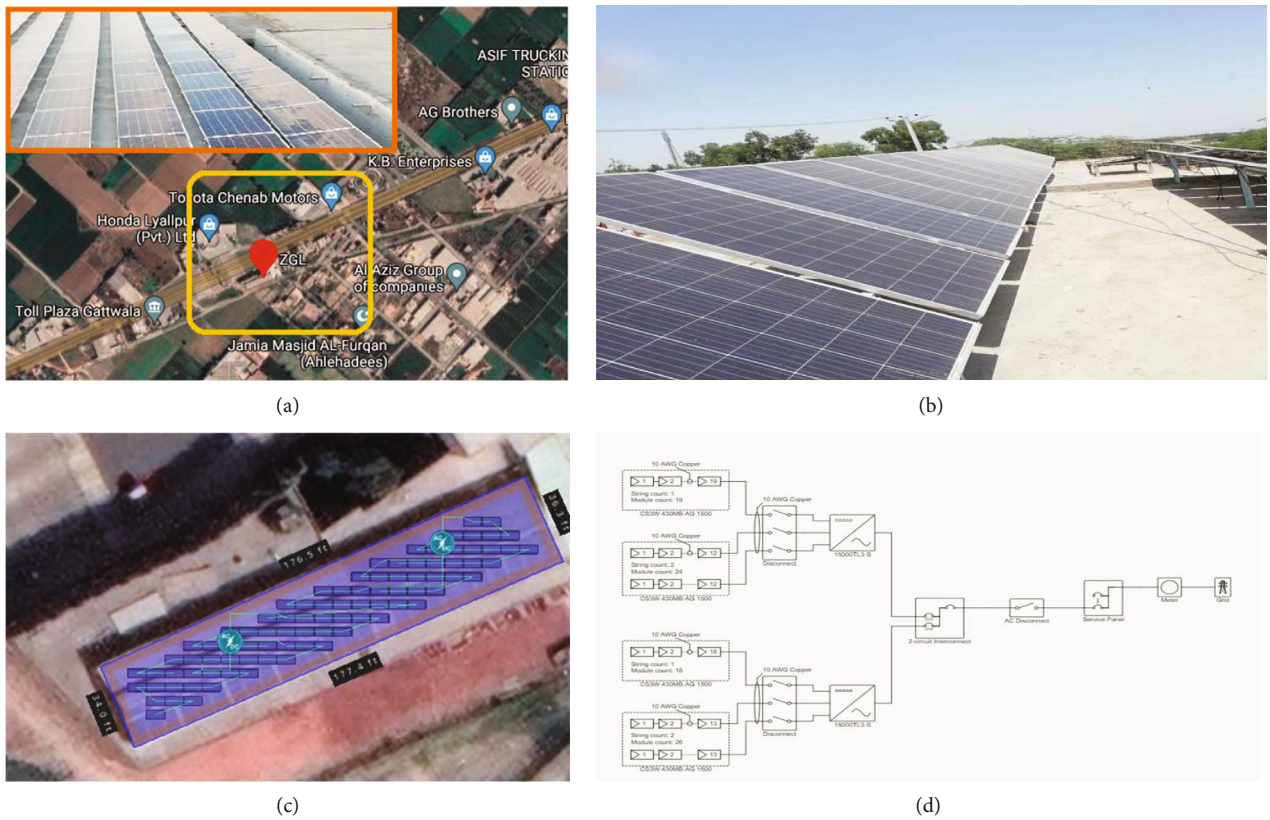

Figure 2: Overview of installed PV system (15 kWp): (a) location on map in Faisalabad; (b) real-time overview; (c) string diagram; (d) single line diagram (SLD).

The monthly average daily values of solar radiation for the region range from 5.5 to 5.8 kWhm^{-2}. Figure 2(a) displays the aerial view of the installed PV systems. The PV systems are installed on the rooftop of a switchgear manufacturing firm, where the top row is designed with monoperk PV modules, and the lower row is designed with polyperk PV modules as depicted in Figure 2(b). These PV plates are supported by a steel stand having tilt angles of 30°. To mitigate the effects of dust accumulation, it is necessary to regularly clean the plates at least once a week [12].

2.1. Types of PV Modules. The capacity of the installed grid-tied PV system is 15 kWp which is composed of two independent monocrystalline and polycrystalline segments. Each segment is installed in a series parallel and has a capacity of 15 kWp. The systems are installed facing south having an optimum monthly tilt angle to enhance their efficiency. In this study, thirty-eight monocrystalline modules (model CS3400WP) and thirty-four polycrystalline modules (model CS3400WP) of similar maximum power output and efficiency ratings are used. Properties of the installed modules are summarized in Table 1. There are four mounting structures of galvanized steel frames holding six panels for each type of PV module. The design of the support structure is to keep a variable inclination with the horizontal plane with the reinforced concrete foundation to withstand the weight of modules and maximum wind speeds at the site as shown in Figure 2(b).

The following formulae can be used for calculating parameters related to the designing of a PV system.

Equations (1) and (2) can be used to calculate the required numbers of PV panels.

$$PV_{\text{Max}} = \frac{Le \times I_P}{H_{\text{Avg}} \eta \text{inv} T_{cf}}, \tag{1}$$

where PV_{max} is the peak power of PV array (kWp), L_e is the electrical load (kWh/day), I_P is the peak solar intensity, H_{Avg} is the average available radiation in kWh/m^2/d, and T_{CF} is the temperature correction factor (0.4-0.5% °C for crystalline silicon) and the efficiency of inverter.

$$PV_N = \frac{\text{PV}_{\text{Max}}}{P_m}, \tag{2}$$

where P_m is the rated power of the selected panel and PV_N is the number of PV panels.

$$\text{Size of inverter} = \text{Total Load} + \frac{\left(1 + A_f\right)}{I_e V_A}, \tag{3}$$

where A_f is the additional further load expansion (20%), I_e is the efficiency of inverter, and V_A is the volt-ampere.

$$P_M = V_M \times I_M, \tag{4}$$

where V_M is the voltage at maximum power point, I_M is the current at maximum power point, and P_M is the maximum power.

Soiling ratio:

$$\text{SRatio}_{\text{measured}} = \frac{P_{m(\text{soiled module})}}{P_m(\text{clean module})} \bullet k_{\text{mismatch}}, \tag{5}$$

where Pm (solid module) is the measured maximum power of the solid module, Pm (Clean module) is the measured maximum power of the clean module, kmismatch quantifies the disparity in Pm between the clean and the soiled modules, and SRatiomeasured compares the measured maximum power (Pm) of the soiled and the clean module.

2.2. Three-Phase Inverters. Since the PV modules are semiconductors in nature, they fundamentally generate direct current (DC). The transmission and distribution systems are designed for AC which is obtained by converting it from DC via inverters and feeds the utility of the electrical grid by synchronized frequency normally around 50 or 60 Hz. The selection of the inverter is based on the maximum output power from each type of PV module array. All inverters are of SolisMax, model Solis-15 K Max; the technical features of the inverters are provided in Table 2.

3. Parameters Considered for the Performance Analysis of Installed PV Systems

Effective and credible assessment of any system's performance is crucial for the designing of an efficient power system. The PV performance is a vital indicator to analyze the quality of its design and reliable combination of PV equipment. According to the International Electrotechnical Commission (IEC) standard 61724, the standard performance parameters for PV-based power systems play a crucial role in the efficiency of a system.

3.1. Final Yield. The definition of the final yield revolves around the portion of total energy generated (E_{EA}) by the whole PV power plant to the rated output power (P_{PV}) per kilowatt of installed PV array during a specified period (i.e., day, month, or year). It can be calculated by

$$\text{Final Yield} = \frac{E_{\text{AC}}}{P_{\text{PV,Rated}}}, \tag{6}$$

where E_{AC} is the total energy generated and P_{PV} is the rated output power.

3.2. Reference Yield. Referenced yield can be defined as the total irradiance (H_t) divided by irradiance (G_{STC}), which, primarily, is 1 kW/m^2 (Equation (7)). This constitutes the solar energy that is available for a specifically mentioned time frame at any place where the PV power system has been deployed. It constitutes the hours per day that are necessary to obtain solar radiation to be at reference irradiance level to produce the same incident energy as received by the sun [25].

$$\text{Reference yield} = \frac{H_t}{G_{\text{stc}}}, \tag{7}$$

where H_t is the total irradiance and G_{stc} is the irradiance.

3.3. Performance Ratio. Performance ratio (PR) is a significant parameter that depends on the PV power plant's geographical location. It is represented by the ratio of energy outputs obtained actually and theoretically over the time of a month or a year as depicted by Equation (8). A high PR value for a grid-connected PV is an indication that the system is efficient and reliable. The overall losses from various

Table 1: Electrical and mechanical parameters of the installed PV modules.

Electrical parameters of PV module	mc-Si	p-Si
Maximum power (P_{max})	400 Wp	440 Wp
Module efficiency (η)	18.11%	19.7%
Maximum power point voltage (V_{mpp})	38.7 V	40.3 V
Current at maximum power point (I_{mpp})	10.34 A	10.92 A
Open-circuit voltage (V_{oc})	47.2 V	48.7 V
Short circuit current (I_{sc})	10.9 A	11.4 A
Module temperature at NOCT (T_{NOCT})	42+3°C	41+3°C
Temp. coefficient of short circuit current (μIsc)	0.05%/°C	0.05%/°C
Temp. coefficient of open-circuit voltage	-0.29%/°C	-0.28%/°C
Temp. coefficient of maximum power	-0.37%/°C	-0.36%/°C
Mechanical properties of PV module		
Number of cells	144	144
Dimensions of cell	2108∗1048∗40 mm	2132∗1048∗30 mm
Operating temperature	-40~85°C	-40~85°C
Weight (kg)	22.4	22.4

Table 2: Electrical datasheet of three-phase inverters.

Input (DC)	
Max. Dc power ($\cos\theta = 1$)	15 KV
Max. input voltage	1000 V
MPP voltage range/rated input voltage	200-800 V
Min. input voltage/initial input voltage	350 V
Max. input current input A/input B	18 A+18 A
Output (AC)	
Rated power (230 V, 50 Hz)	15 kW
Max. apparent AC power	33 kVA
Rated power frequency	50/60 Hz
Max. output current	21.7 A
Power factor at rated power	0.8 (min.)
Maximum efficiency	97.5%
General data	
Weight	30 KG
Operating temperature range	-26°C~60°C
Noise emission (typical)	<30 dBA
Self-consumption (night)	<1 watt (night)
Topology	Transformer less
Cooling concept	Natural convection

factors such as inverter losses, module mismatch, wiring, temperature, and dust or snow on the rated output power are less. The overall efficiency of the solar photovoltaic power system is closely related to the value of the performance ratio, i.e., closer to 100% [25].

$$\text{Performance ratio} = \frac{Y_f}{Y_r}, \tag{8}$$

where Y_f is the actual energy output and Y_r is the theoretical energy output.

3.4. Capacity Factor. The capacity factor is mainly the ratio of produced electricity capacity factor. Geothermal energy and biomass among the clean and renewable energies perform at higher capacity factors compared to intermittent renewable sources which tend to have lower capacity factors. For PV plants, the capacity factor ranges from 10% to 30%, as their outputs fluctuate resulting from weather conditions [25]. It can be calculated by using

$$\text{Capacity factor} = \frac{Y_f}{\text{hours}}, \tag{9}$$

where Y_f is the actual energy output.

3.5. Meteorological Data. To examine the performance of the PV system, it is required to study the weather data recorded by the weather station. This may include data set comprising temperature and wind speed. The ambient and module temperature fluctuated during the nominated period from November 2020 to August 2021 individually. Undesirable module temperature was usually observed during nighttime. During the measured period, wind velocity varied from 1 ms^{-1} in January and 2 ms^{-1} in June on average, whereas relative humidity reached almost 87% level during the monsoon season (i.e., July and August), and the maximum value of global-tilt solar irradiation of 1225 Wm^{-2} was recorded for Faisalabad. It has been observed that on any sunny day, the module performance is affected by three meteorological parameters. These factors include temperature, solar irradiation, and wind speed, whereas other parameters are shown in Table 3.

Table 3: Meteorological data for Faisalabad.

Parameter measured	Value obtained
Measuring range	0.0-1400.0Wm^{-2}
Resolution	<1Wm^{-2}
Spectral range	300-2800nm
Sensitivity range	5-20μv/Wm^{-2}
Operating temperature rate	-40°C to+80°C
Maximum operational irradiance	2000Wm^{-2}
Relative humidity range	4.35-17.4 Psi
Relative humidity accuracy	±2%RH
Air temperature range	-50°C to +60°C
Air temperature accuracy	0.5°C
Wind speed range	0.8-40m^{-2}
Wind speed measuring accuracy	±0.5%

4. Performance Analysis and Result Discussion

This comparative study visualizes that in winter, the efficiency of monoperk is better as compared to other types of modules. In summer, polyperk performed with better efficiency because it is highly efficient in the high-temperature range. The maximum production of kWh in winters was more than 2,100 kWh for polyperk. The data obtained displayed that the annual average of daily final yield, performance ratio, and capacity factor for 15 kW polyperk was estimated to be 61.94 kWh, 84.17%, and 19.12, respectively. The annual average of daily final yield, performance ratio, and capacity factor for 15 kW monoperk was estimated to be 58.32 kWh, 81.42%, and 18.13, respectively. The reported results are comparatively better than a similar study conducted in Iran [26].

On the other hand, a maximum yield of around 1,700 kWh was obtained from monoperk as summer ambient temperature is high leading to reduced efficiency. At the start of November, the ambient temperature began to decrease, and thus, the efficiency of monoperk also increased, whereas the efficiency of polyperk started decreasing till December as the highest temperature of the season was monitored this month. In March, the yield of monoperk plummeted, whereas for the polyperk modules, the yield improved. In April, May, June, and July, the ambient temperature stayed at a peak level. Therefore, the efficiency of polyperk increased, and consequently, the efficiency of monoperk decreased. In August, temperature variation was observed due to the monsoon season. On warm days, the efficiency of polyperk increased whereas, on the other hand, the efficiency of monoperk increased on relatively cool days as depicted by simulation results in Figure 3(b). So, it can be concluded that polyperk modules outperform monoperk type modules when the ambient temperature increases. The common material used in solar cells, crystalline silicon, does not help to prevent them from getting hot either. As a great conductor of heat, silicon actually speeds up the heat building up in solar cells on hot summer days. Mono PV modules are made from a single crystal of silicon whereas poly is made from several fragments of silicon melted together which prevents it from heating up.

As it can be seen in Figure 3(a), HelioScope-based system generated higher power in comparison to a real-time system as the software considers ideal conditions and ignores various factors that affect the real system output performance such as dust losses and shadow factor.

Scatter plot in Figure 4 displays two hotspots and distinct regions highlighted by two circles. The upper-end circle has a wide range of experimental mono- and polycrystalline systems and polyperk simulation yield results. The lower circle has a keen distribution of yield results in experimental monocrystalline systems and polyperk simulated systems. Only peculiar results in raw data for the distinctive monocrystalline solar energy material produce oblique and relatively lesser in midseason.

Quantified data and behavior in tail line circles need to be categorized using learning, training, and testing data sets for relative comparison, which is a new theme in solar energy system classification; further details are defined in Section 4.

Ideal conditions and real-time working systems classify two different data sets and elucidated graphs. Statistical graphs show the relatively higher difference in total yield over the time scale length in real time due to undistinguished and random errors in calculations and measurement. Figure 4 shows the hotspot regions using the estimated data varying from lower tail to high end. Figures 5 and 6 depict raw data sets in peak slope form. Figures 4 and 5 show distinct groups and variations in estimated and calculated values. In polyperk system experimentation, Figure 6 shows the error doping in mean values for polyperk crystalline modules (simulation and experiment result comparison). A greater mean error exists in the experimentation results with the range lying in 1250 to 1470 kWh in comparison to simulation results with the least mean error in the upper bound of 1950 kWh. Significance of new advance predictive and artificial intelligence tools in the realm of statistical-based machine learning produces a counterproductive approach using both real-time and ideal simulation patterns and data sets for classification and decision-making for applied applications while using monoperk and polyperk solar systems. The apparent results are statistically plotted for heat mapping to understand the relationship between the distinctive classes of monoperk and polyperk crystalline modules of simulation and experimental data sets.

Figures 7 and 8 display futuristic parameters that are independent and dependent in nature on each other. Plasma-type heat map of monoperk crystalline modules shows maximum nonlinearity in the experimental and simulation results up to -0.86. The corresponding increase in module yield is inferred from the heat map but linearity is minimum in experimental and simulation results with values as low as 0.14 and 0.16. In polyperk crystalline modules, greater amount of synergy is accounted for in the experimental and simulation results. The corresponding results are accounted for and validated with heat map-linearity values greater than monoperk crystalline modules up to ~0.98. However, in relationship with months and

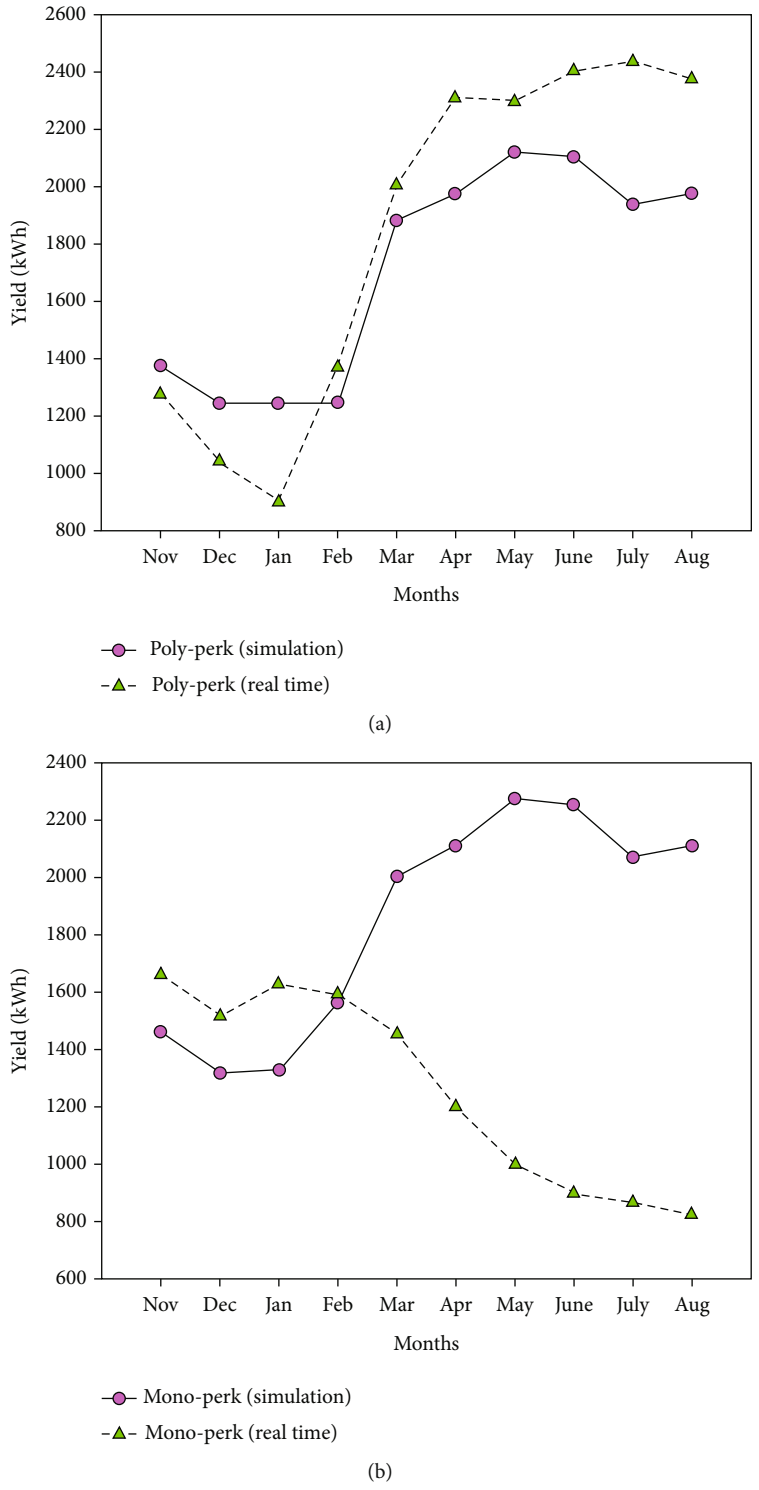

Figure 3: Comparison of yield obtained from simulation and real-time systems: (a) yield obtained from polyperk PV modules; (b) yield obtained from monoperk PV modules.

method classes, a reverse effect has been observed with negative values of as low as -0.061 and -0.96 for experimental and simulation data sets.

Heat maps in Figures 7 and 8 depict the statistical difference with nonlinearity and class distinction. An efficient technique must be applied for validating results, consolidating decisions for which type of crystalline modules and which method needs to be implemented for desirable calculation of yield measurement according to our requirements. Machine learning algorithms are statistically powerful

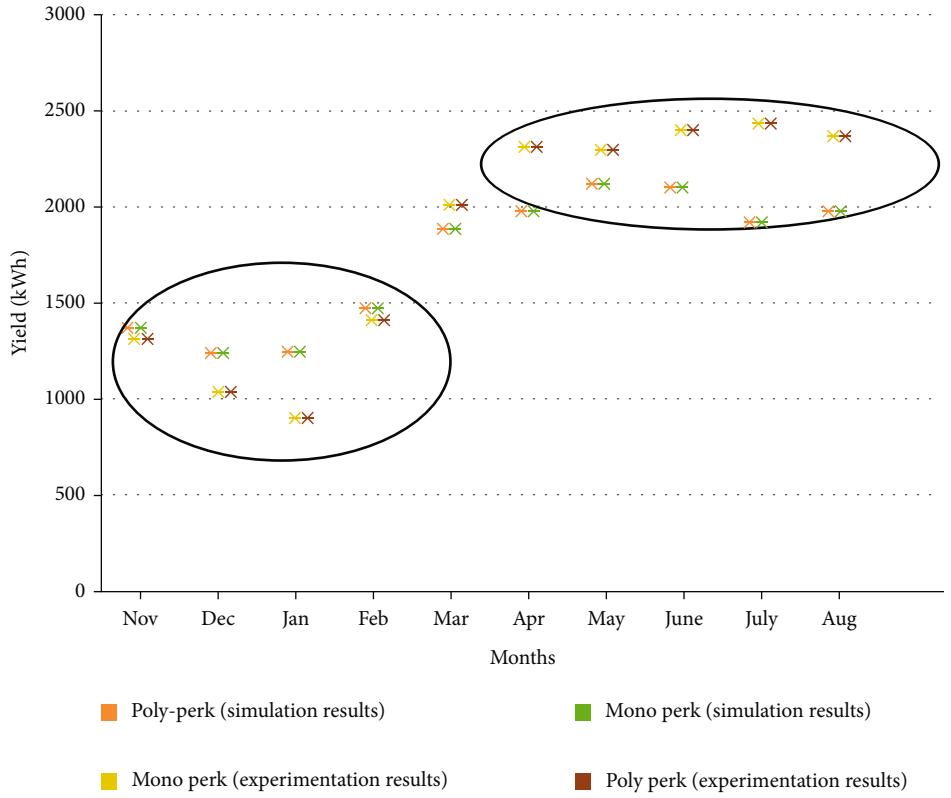

Figure 4: Comparison of hotspots generated by mono- and polyperk on monthly basis using real-time installed systems and simulations.

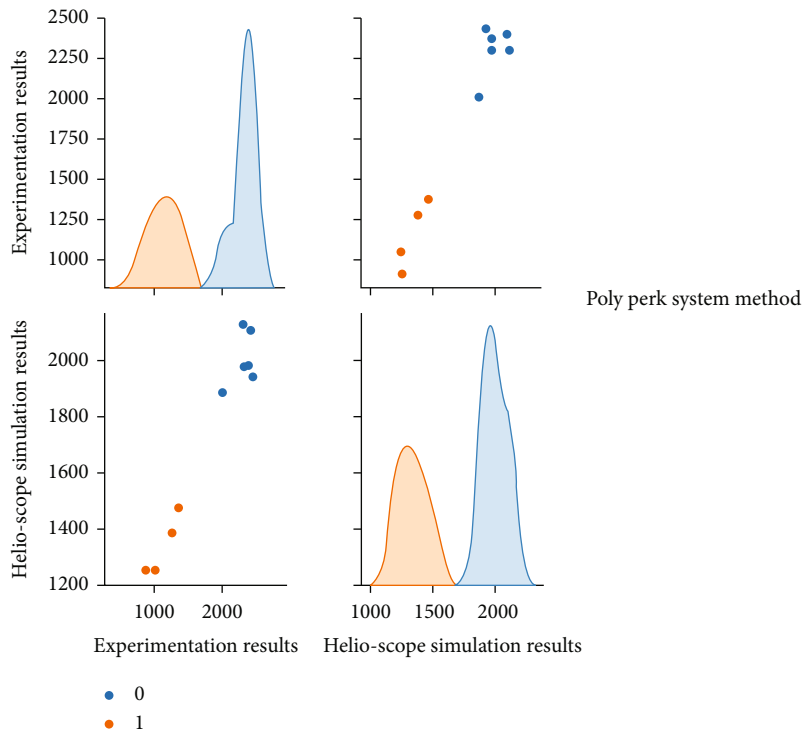

Figure 5: Peak form data of experimental and simulation results for polycrystalline material energy systems (1, simulation; 0, experimentation).

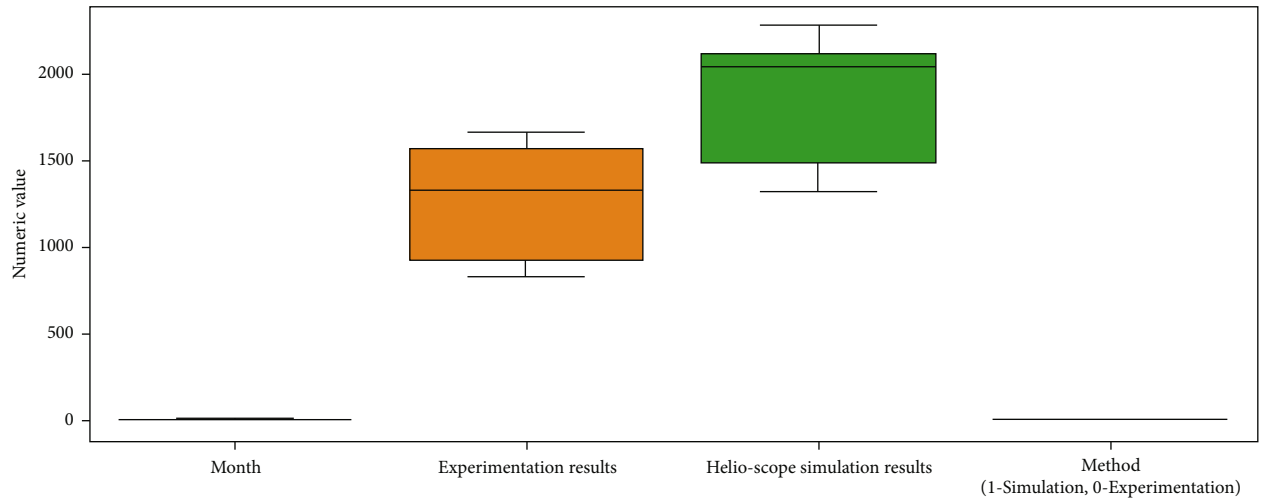

Figure 6: Mean error-box plot using Seaborn library of experimental and simulation result data for mono- and polycrystalline material energy systems.

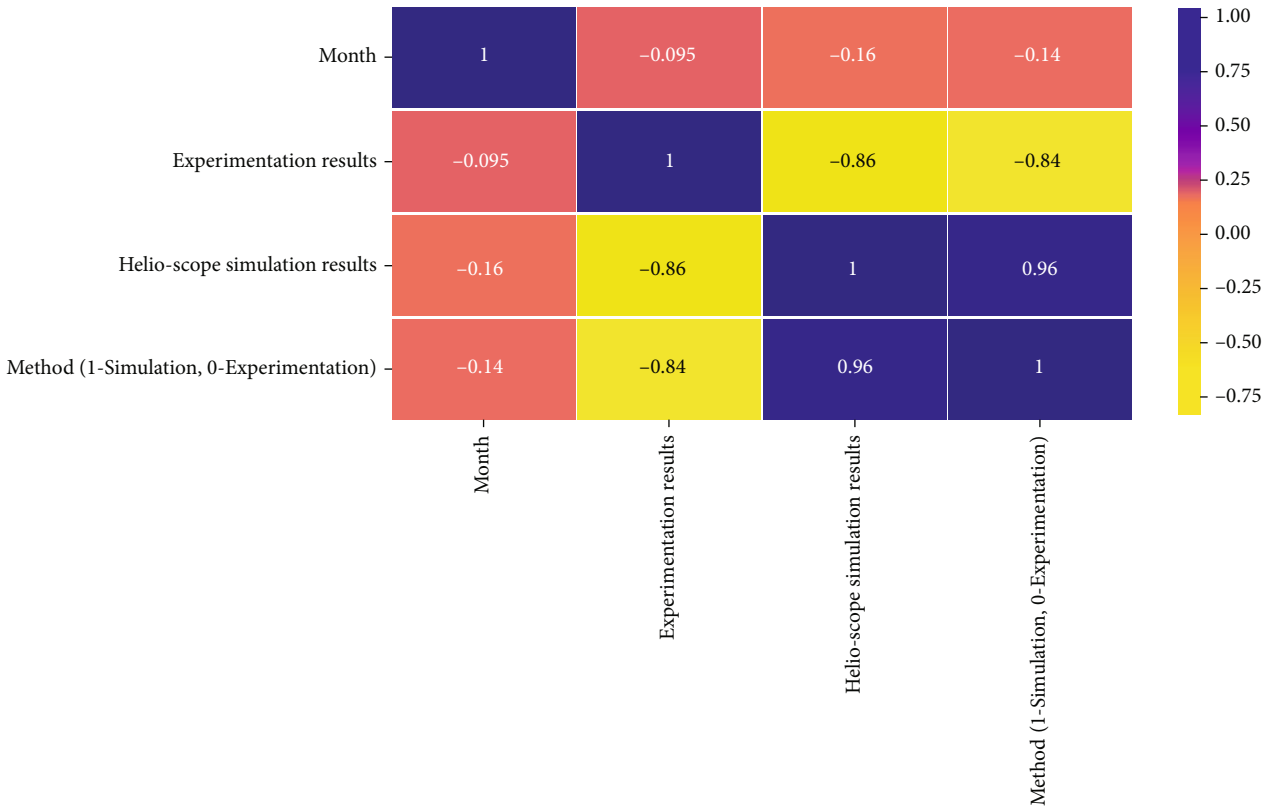

Figure 7: Heat map between each independent and dependent variable in case of monoperk crystalline modules.

algorithms that over the period of using artificial intelligence learning update their sets and make the logical decision of either using experimental means or simulation for time and cost-saving.

4.1. Machine Learning-Based Relative Performance Investigation of Mono- and Polyperk Modules. As previously defined, the nonlinearity and class distinction in the available raw data sets are classically classified into the categorical division between experimental and simulation results. Parametric results of machine learning-based logistical regression have been introduced as a strategic machine learning algorithm due to its robust nature and easiness with mixed data set performance. Using this technique, the algorithm will

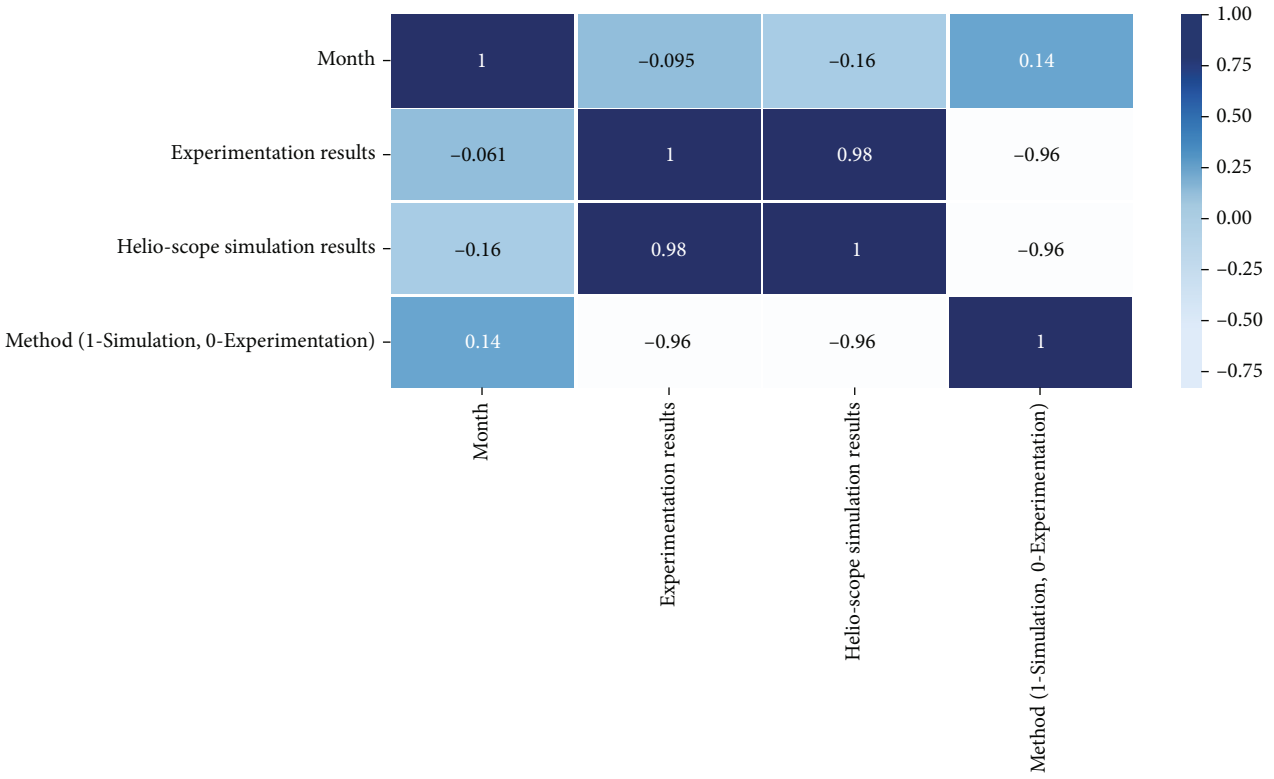

Figure 8: Heat map between each independent and dependent variable in the case of polyperk crystalline modules.

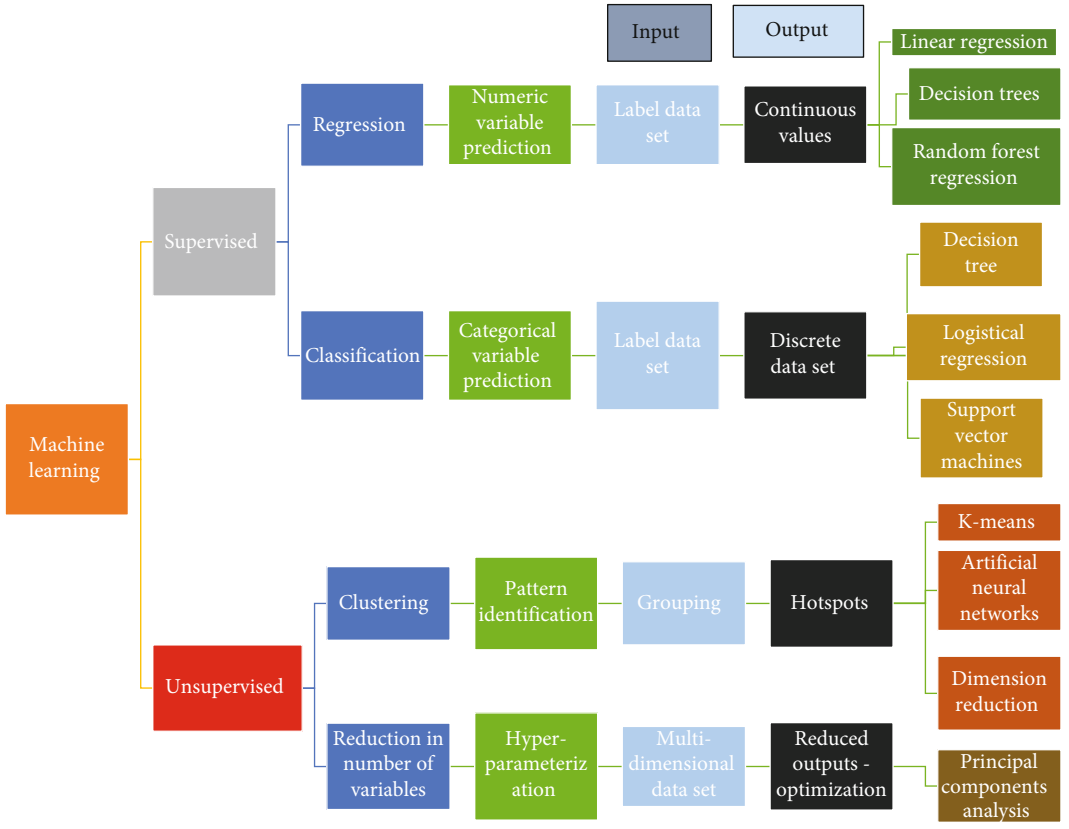

Figure 9: Machine learning algorithms and flow chart.

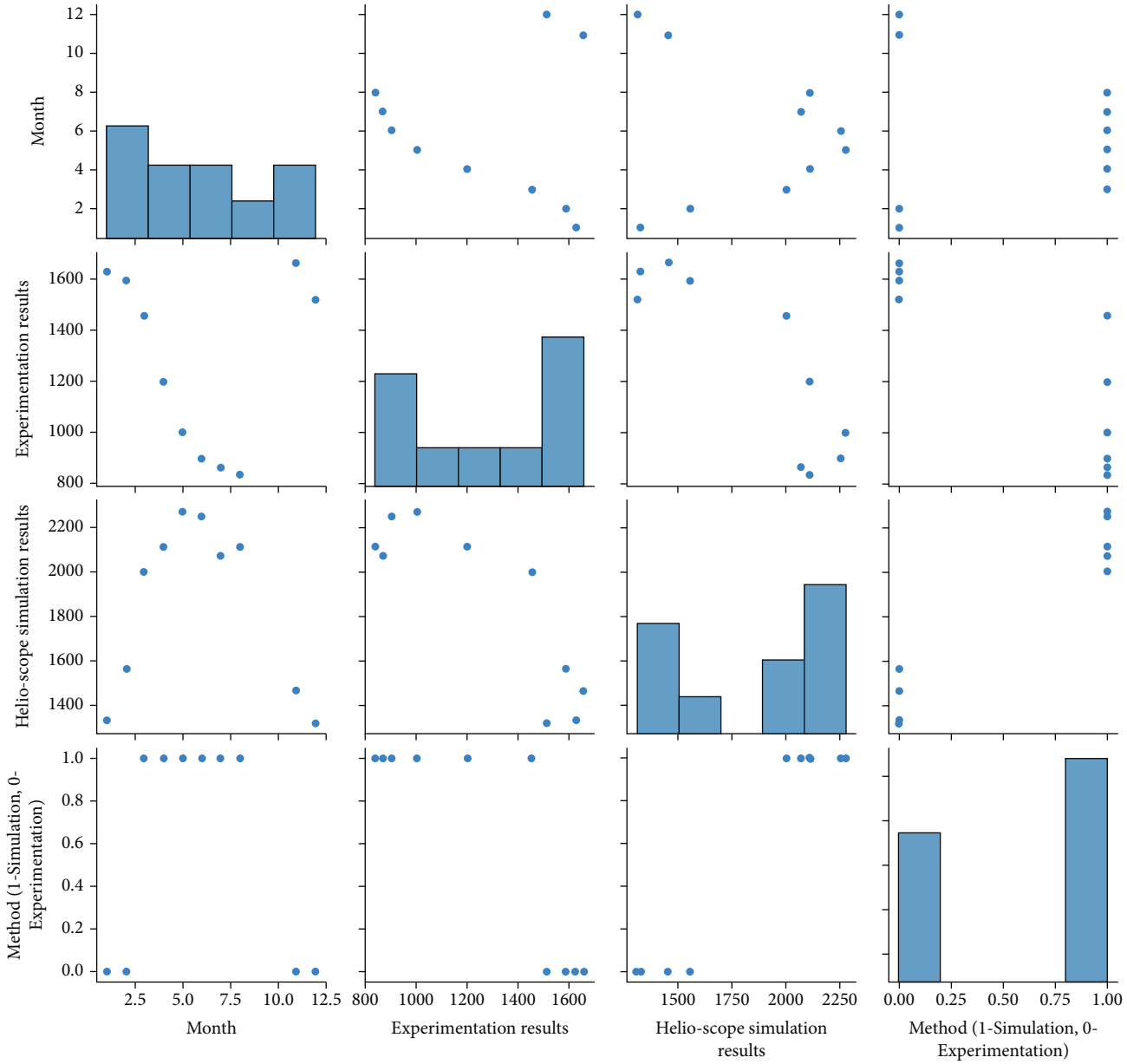

Figure 10: Pair plot of monoperk module data sets in grid-connected formation for correlation between each independent and dependent variable.

evaluate the reasons behind the performance gap between simulation and real-time system outputs as shown in Figure 3 and help to contain the error to a minimum; it also provides useful insight, corelation, and evaluation with class distinction according to subjective weather and time horizon.

4.1.1. Machine Learning-Based Logistic Regression Modeling. Machine learning- (ML-) based regressions are keenly a new method for inference of error and hyperparameter deduction. For efficient future predictive system installation, result synchronization, and error reduction between the simulation model and real-time system, machine learning-based logistic regression modeling has been performed in this section. ML classification has been done on the following three algorithms:

(1) Supervised learning

(2) Unsupervised learning

(3) Reinforcement learning

Flowchart classification of machine classes, input and output data set nature, and algorithms are presented in Figure 9.

The categorical data in ML lies mainly in the domain of logistic regression. Linear and polynomial regressions are commonly used for conventional regressive weight

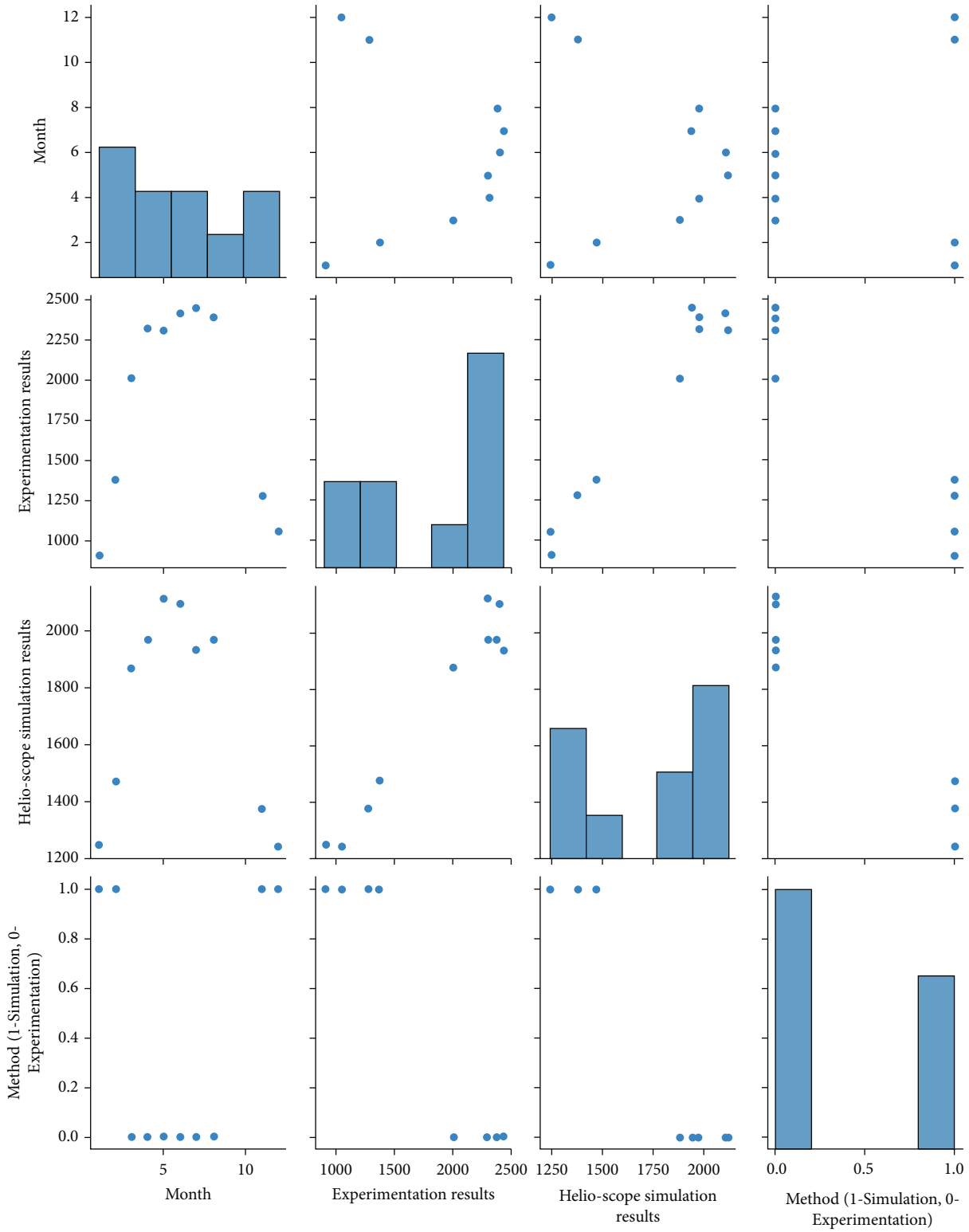

Figure 11: Pair plot of polyperk module data sets in grid-connected formation for correlation between each independent and dependent variable.

parameters and their corelations based on p values. ML differentiates logistical regression from linear regression based on the continuous and descriptive data set, respectively. The regular fit in linear regression mainly highlights continuous values in a data set. Logistic regression predicts whether something is either true or false, yes or no, and 1 or 0, instead of predicting the weight or performance based on the mean absolute, R^2, etc., values. Due to

significant differences between the simulation results and experimental results performed earlier and as highlighted by statistical values, i.e., the standard error lies in-between 5 and 45% for polyperk crystalline and 5 and 25% for Monocrystalline PV grid-connected module. ML-based logistic regression modeling has been carried out. A pair plot drawn in Python using the Seaborn library assimilates the finest set of attributes and features for a relative explanation of relationships between two and more variables. The plot displays clusters and separation of offset data points along with hyperparameters that results in decision-making and classification of either supervised or unsupervised algorithm for machine learning. Pair plots in Figures 10 and 11 show class representations in monoperk and polyperk module data sets with bar plots showing energy yield produced over a time series.

Monoperk crystalline grid-connected system shows the sigmoidal plot and two hotspot regions mainly featuring yield and timeline variable, i.e., month. Figures 10 and 11 also depict method validity for the experimentation and simulation results. The pair plot of monoperk has data sets more aligned statistically for simulation data and interpretations, while the polyperk features data more viable within experimentation data points. The pair plot consists of scatter plots and bar plots. Experimentation data points in the pair plot depict a higher yield for polyperk as compared to the monoperk crystalline grid-connected system.

The under discussion ML-based case study for monoperk and polyperk crystalline module-based grid-tied systems is being conducted first time as no previous literature is available regarding the AI-based performance analysis. This method highlights the significance of implications between simulated and experimental methods with error reduction, consolidation, and the performance evaluation of grid-tied PV solar modules.

Anaconda-Python 3.8 libraries including NumPy, Matplotlib, Seaborn, pandas, and scikit-learn have been utilized for data analysis and machine learning-based decision modeling between experimental and simulation results. The initial case study for the polyperk crystalline module data set shows a higher error doping in mean values during experimental evaluation in comparison to simulation results as shown in Figure 5.

Figure 5 displays the comparison based on error occurrence between simulation and experimental results in the polyperk crystalline module where class 0 represents experimental and class 1 represents simulation results. In both simulated and experimental environments, per month yield maximum output has been calculated. The descriptive statistics of the polyperk and monoperk crystalline PV module performance can be seen in Tables 4 and 5.

It can be seen from the extracted features represented in Tables 4 and 5 that there is a significant difference between simulation and experimental data. This difference is due to the ideal scenario of the software as there is no consideration of temperature variance and its effect on the system performance as well as other factors such as dust factor and shadow factor. Based on the abovementioned features, a machine learning algorithm has been used to signify the error reduction and predictability module.

Table 4: Statistics (extracted features) based on performance analysis of polyperk modules.

Features	Experimental values	Simulated values
Mean	1842.98	1733.76
Standard error	196.6675	112.8729366
Median	2152.85	1909.65
Standard deviation	621.9171	356.9355659
Sample variance	386780.9	127402.9982
Kurtosis	-1.78782	-1.825932887
Skewness	-0.51473	-0.450257756
Range	1537.4	879.6
Minimum	900.8	1243
Maximum	2438.2	2122.6
Sum	18429.8	17337.6
Count	10	10
Largest (1)	2438.2	2122.6
Smallest (1)	900.8	1243
Confidence level (95.0%)	444.8927	255.3363221

Table 5: Statistics (extracted features) based on performance analysis of monoperk modules.

Features	Experimental values	Simulated values
Mean	1265.67	1849.62
Standard error	108.0271232	122.1181821
Median	1328.6	2037.5
Standard deviation	341.6117584	386.1715992
Sample variance	116698.5934	149128.504
Kurtosis	-2.063216661	-1.835603662
Skewness	-0.155217059	-0.435316653
Range	827.7	957.9
Minimum	834.6	1317.3
Maximum	1662.3	2275.2
Sum	12656.7	18496.2
Count	10	10
Largest (1)	1662.3	2275.2
Smallest (1)	834.6	1317.3
Confidence level (95.0%)	244.3743305	276.2505204

4.1.2. Logistical Regression Mathematical Representation. Logistical regression is generally used for two-class problems and can be extended for implications in the multiclass problems but becomes highly unstable in calculations when classes are well separated; the working diagram is represented in Figure 12. The baseline for the mathematical formulation of logistical regression is simple linear regression.

$$y = b_o + b_1 x, \tag{10}$$

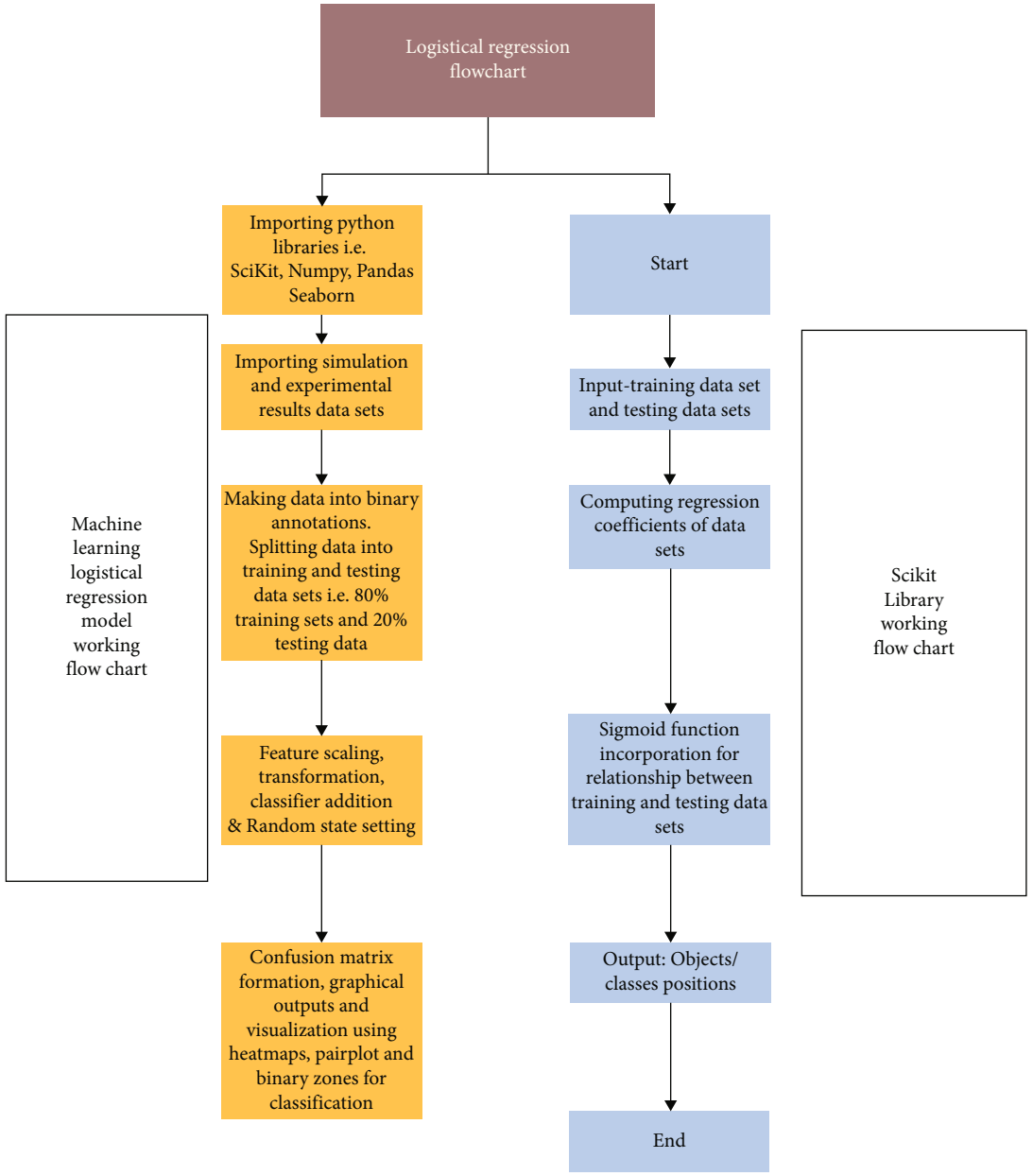

Figure 12: Working diagram of the testing and training in logistical machine learning regression modeling.

where y is the continuous output result while the b_o is the intercept of the line, b_1 is the slope of the line, and x is the input or independent variable. In continuous data, we can utilize linear regression, but in distinct classes, we cannot draw the best-fit curve. We introduce a classifier for whether an action/event shall occur or not. Figure 13 shows that the output in logistical regression is binomial. LR has a sigmoid function based on the probability of an event (P) and ranges from 0 to 1 and is given as

$$P = \frac{1}{(1 + e^{-y})}. \tag{11}$$

Introducing P in the LR equation and computing at the natural log scale gives the following mathematical expression:

$$\ln\left(\frac{P}{1-P}\right) = b_o + b_1 x. \tag{12}$$

Weighted output is in the range of either 0 or 1; if the output is <0.5, then it corresponds to 0th class if not then 1st class. For training and testing data sets after incorporation into machine learning the module, accuracy is defined by

$$\text{Accuracy}\,(\%) = \frac{\text{Corrrect Predictions}}{\text{Total Predictions}} \times 100\%. \tag{13}$$

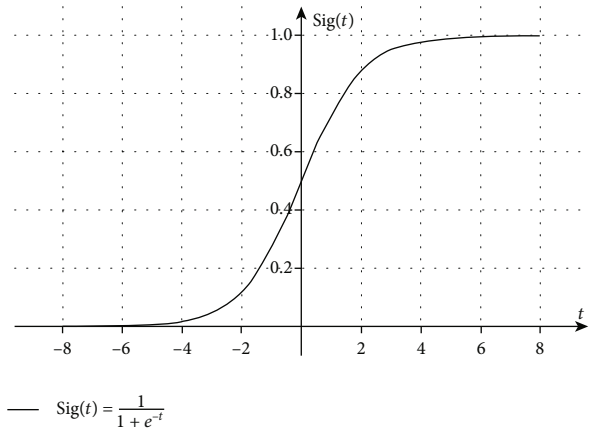

Figure 13: Sigmoid function behavior at a discrete event time scale length.

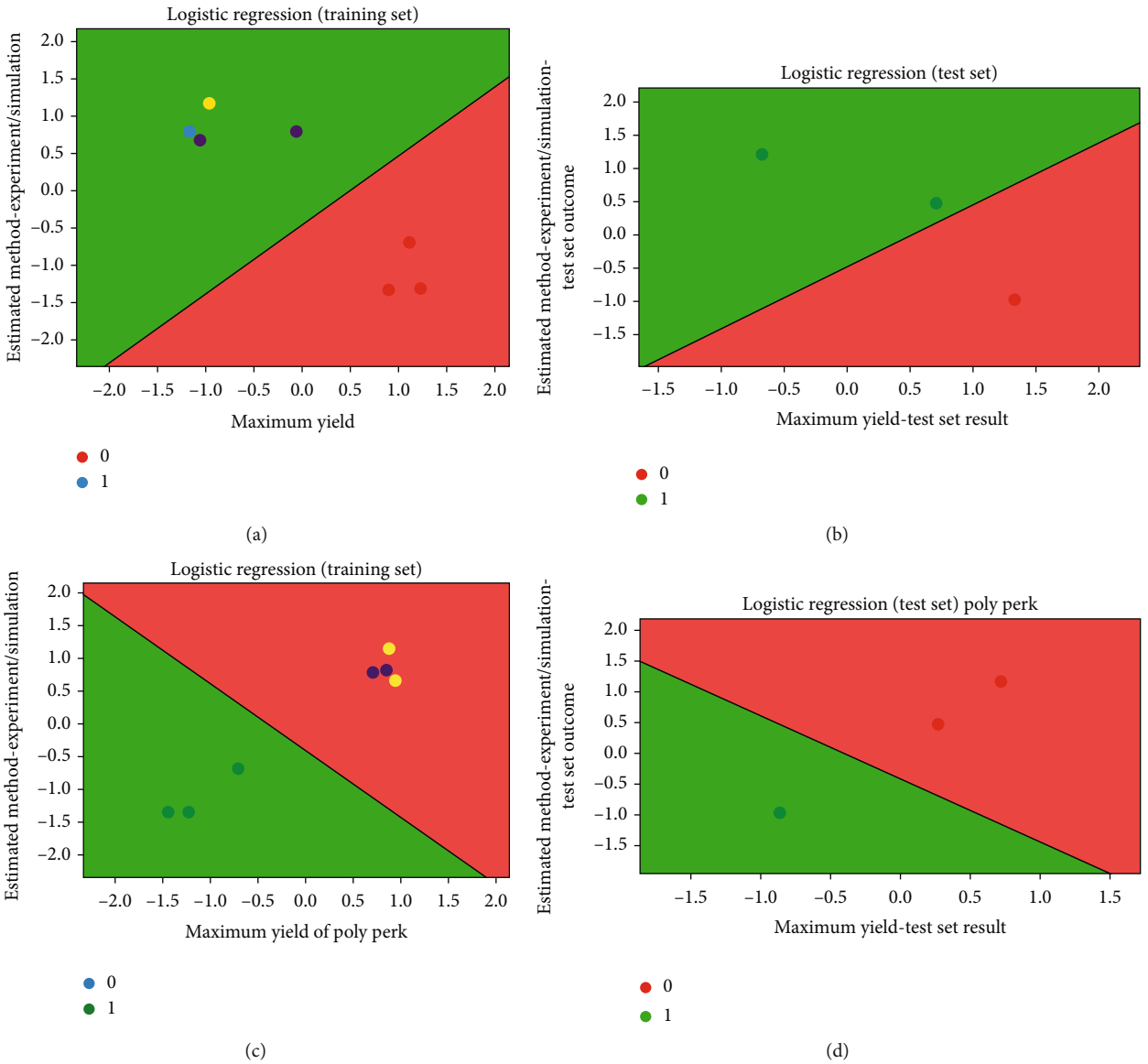

Figure 14: Working data sets of monoperk and polyperk modules using logistic regression: (a) training set of monoperk module; (b) testing set of monoperk module; (c) training set of polyperk module; (d) training set of polyperk module.

Table 6: Data set of monoperk crystalline module in simulation and experimental work.

Month	Monoperk experimental results	Monoperk simulation results	Method/class max. yield output	Difference	Error percentage
January	1629.5	1329	0	300.5	18.44123964
February	1591	1561	0	30	1.885606537
March	1456.5	2003.5	1	547	27.30222111
April	1200.7	2110.7	1	910	43.11365898
May	1000.2	2275.2	1	1275	56.03902954
June	899.1	2254.1	1	1355	60.11268355
July	865.5	2071.5	1	1206	58.21868211
August	834.6	2111.6	1	1277	60.47546884
November	1662.3	1462.3	0	200	12.03152259
December	1517.3	1317.3	0	200	13.1813089

Table 7: Data set of polyperk crystalline module in simulation and experimental work.

Month	Experimental polyperk results	Polyperk simulation results	Method/class max. yield output	Difference	Error percentage
January	900.8	1245.8	1	345	27.69304864
February	1371.2	1471.2	1	100	6.797172376
March	2007.1	1881.1	0	126	6.277714115
April	2311.1	1976.1	0	335	14.495262
May	2298.6	2122.6	0	176	7.656834595
June	2405.6	2105.6	0	300	12.47090123
July	2438.2	1938.2	0	500	20.50693134
August	2377.5	1977.5	0	400	16.82439537
November	1276.5	1376.5	1	100	7.264802034
December	1043.2	1243	1	199.8	16.07401448

The accuracy of a system based on the prediction of classification problems is either correct or can be incorrect so a matrix, namely, a confusion matrix, is formed for a relational summary of actual and predicted values of classification problems.

4.1.3. Performance Analysis of Mono- and Polyperk Crystalline Modules. The total reading count of simulation and experimental work is divided into 80% training and 20% testing data as shown in Figure 14. The classifier is introduced for encoding purposes to have the binary distinction between greater probability events. The timeline horizon consists of 10 months; no data was conceived for the month of September and October.

$$\log(p) = \ln \frac{p}{(1-p)1-p}, \tag{14}$$

where P is the probability of a discrete event defined earlier.

The training data set selects a total of 80% values from raw data. The algorithm reads the pattern according to the problem statement and improves the probability values. In each run, a class check is run for appointing the new red and green distribution as highlighted in Figure 14. An increase in the iterations increases the width of class boundaries. Based on the extracted features and training/testing of both modules, the data set collected from simulation and experimental work of mono- and polyperk crystalline module for a one-year cycle (except September and October) can be seen in Tables 6 and 7 which depict the difference between them ranging from 1% to 60.5% in monoperk and 6% to 27% in polyperk crystalline.

In logistical regression training, the data set values determine the probable event in advance. The most likelihood and unlikelihood are distinguished for experimental and simulation results. For the monoperk crystalline grid-connected system in the experimental scenario, readings are likelihood, and the probability after training and testing the data set lies about 99% accuracy. The confusion matrix produces an absolute validated summary result for the method and material to be incorporated in each particular scenario. A 20% test data set values in most actual and predicted values are in harmony with each other using the ML module. In further classification, as shown in the heat map and pair plot in Figures 8–11, the class distinction reflects that those major values classified in the experimental work are authentic.

To determine the evaluation of the monoperk crystalline grid-connected system, experimental work is more reliable than compared to a simulation study. The error difference reduces in off-peak months of the data cycle, i.e., January, February, and March, whereas in peak months, the

evaluation results are likely the same and coherent. In the case of polyperk crystalline grid-connected studies, a greater significance and accuracy lies within the simulation and experimental studies, and the likelihood of probability is significant as seen in Tables 6 and 7. Model accuracy after training and testing produces results of up to 99.5%. Simulation results are likely most favorable in predicting the performance evaluation of maximum yield in grid-connected systems. During off-peak (i.e., winter season), the error difference increases due to various factors such as module angle, line losses, cell dimension, and temperature invariability.

5. Conclusions

In this research, a comparative study was conducted for two solar systems of 15 kW. The systems primarily included monoperk and polyperk crystalline. From the study, it was observed that maximum yield was produced, in winters, by monoperk, while during summers, polyperk displayed enhanced efficiency. In Faisalabad, polyperk has proven to be efficient considering the high rates of temperature whereas monoperk, consequently, reduced the efficiency of the solar system. The annual average of daily final yield, performance ratio, and capacity factor for 15 kW polyperk was estimated to be 61.94 kWh, 84.17%, and 19.12, respectively. The annual average of daily final yield, performance ratio, and capacity factor for 15 kW monoperk was estimated to be 58.32 kWh, 81.42%, and 18.13, respectively. The efficiency can also be attributed to the quality of the system. For example, good quality inverter requires quality plates for enhanced efficiency. Additionally, the production of a 430-watt panel was noted as 400 watts. Furthermore, according to the applied machine learning module, a significant difference was observed in the considered PV module types (i.e., mono- and polyperk). A machine learning modeling study using logistical regression was applied to determine the greater significance of experimentation results in monoperk crystalline with an accuracy of 99.5%, while the results in polyperk using simulation studies are more accurate and recommended in the evaluation of PV-connected grid. Depending upon observed parameters and frequency period, the model elucidated a better understanding of the performed real-time analysis leading to both cost and time saving for the installation of similar projects in the region. Furthermore, better performance can be achieved from installed systems if factors such as dust, tilt angle, and shadow effects are considered before the installation of PV systems.

Data Availability

Data will be available on request. For data-related queries, kindly contact Faisal Mahmood (faisal.mahmood@uaf.edu.pk).

Conflicts of Interest

The authors declare that there is no conflict of interest regarding the publication of this research article.

Acknowledgments

The authors acknowledge the support of the Department of Energy Systems Engineering and Punjab Bio-Energy Institute (PBI), University of Agriculture, Faisalabad, for facilitating data collection. This work was supported by the Korea Institute of Planning and Evaluation for Technology in Food, Agriculture and Forestry (IPET) through the Technology Commercialization Support Program, funded by the Ministry of Agriculture, Food and Rural Affairs (MAFRA) (No. 821048-3).

References

[1] Government of Pakistan Finance Division, "Pakistan economic survey," 2019, https://www.finance.gov.pk/survey_1920.html.

[2] M. S. Adaramola and E. E. T. Vågnes, "Preliminary assessment of a small-scale rooftop PV-grid tied in Norwegian climatic conditions," *Energy Conversion and Management*, vol. 90, no. 2015, pp. 458–465, 2015.

[3] L. M. Ayompe, A. Duffy, S. J. McCormack, and M. Conlon, "Measured performance of a 1.72kW rooftop grid connected photovoltaic system in Ireland," *Energy Conversion and Management*, vol. 52, no. 2, pp. 816–825, 2011.

[4] G. C. Bakos, "Distributed power generation: a case study of small scale PV power plant in Greece," *Applied Energy*, vol. 86, no. 9, pp. 1757–1766, 2009.

[5] D. Chemisana and C. Lamnatou, "Photovoltaic-green roofs: an experimental evaluation of system performance," *Applied Energy*, vol. 119, pp. 246–256, 2014.

[6] P. Ferrada, F. Araya, A. Marzo, and E. Fuentealba, "Performance analysis of photovoltaic systems of two different technologies in a coastal desert climate zone of Chile," *Solar Energy*, vol. 114, pp. 356–363, 2015.

[7] T. Khatib, K. Sopian, and H. A. Kazem, "Actual performance and characteristic of a grid connected photovoltaic power system in the tropics: a short term evaluation," *Energy Conversion and Management*, vol. 71, pp. 115–119, 2013.

[8] A. H. A. Al-Waeli, M. T. Chaichan, H. A. Kazem, K. Sopian, and J. Safaei, "Numerical study on the effect of operating nanofluids of photovoltaic thermal system (PV/T) on the convective heat transfer," *Case Studies in Thermal Engineering*, vol. 12, pp. 405–413, 2018.

[9] A. H. Al-Waeli, H. A. Kazem, K. Sopian, and M. T. Chaichan, "Techno-economical assessment of grid connected PV/T using nanoparticles and water as base-fluid systems in Malaysia," *International Journal of Sustainable Energy*, vol. 37, no. 6, pp. 558–575, 2018.

[10] H. A. Kazem, J. Yousif, M. T. Chaichan, and A. H. Al-Waeli, "Experimental and deep learning artificial neural network approach for evaluating grid-connected photovoltaic systems," *International Journal of Energy Research*, vol. 43, no. 14, pp. 8572–8591, 2019.

[11] J. Y. Kim, G. Y. Jeon, and W. H. Hong, "The performance and economical analysis of grid-connected photovoltaic systems in Daegu, Korea," *Applied Energy*, vol. 86, no. 2, pp. 265–272, 2009.

[12] K. A. Kumar, K. Sundareswaran, and P. R. Venkateswaran, "Performance study on a grid connected 20 kW p solar photovoltaic installation in an industry in Tiruchirappalli (India),"

Energy for Sustainable Development, vol. 23, pp. 294–304, 2014.

[13] D. H. W. Li, K. L. Cheung, T. N. T. Lam, and W. W. H. Chan, "A study of grid-connected photovoltaic (PV) system in Hong Kong," *Applied Energy*, vol. 90, no. 1, pp. 122–127, 2012.

[14] K. Padmavathi and S. A. Daniel, "Performance analysis of a 3MWp grid connected solar photovoltaic power plant in India," *Energy for Sustainable Development*, vol. 17, no. 6, pp. 615–625, 2013.

[15] V. Sharma, A. Kumar, O. S. Sastry, and S. S. Chandel, "Performance assessment of different solar photovoltaic technologies under similar outdoor conditions," *Energy*, vol. 58, pp. 511–518, 2013.

[16] V. Sharma and S. S. Chandel, "Performance analysis of a 190 kWp grid interactive solar photovoltaic power plant in India," *Energy*, vol. 55, pp. 476–485, 2013.

[17] Y. Su, L. C. Chan, L. Shu, and K. L. Tsui, "Real-time prediction models for output power and efficiency of grid-connected solar photovoltaic systems," *Applied Energy*, vol. 93, pp. 319–326, 2012.

[18] X. Wu, Y. Liu, J. Xu et al., "Monitoring the performance of the building attached photovoltaic (BAPV) system in Shanghai," *Energy and Buildings*, vol. 88, pp. 174–182, 2015.

[19] W. Zhou, H. Yang, and Z. Fang, "A novel model for photovoltaic array performance prediction," *Applied Energy*, vol. 84, no. 12, pp. 1187–1198, 2007.

[20] M. Mani and R. Pillai, "Impact of dust on solar photovoltaic (PV) performance: research status, challenges and recommendations," *Renewable and Sustainable Energy Reviews*, vol. 14, no. 9, pp. 3124–3131, 2010.

[21] A. Y. Appiah, X. Zhang, B. B. K. Ayawli, and F. Kyeremeh, "Review and performance evaluation of photovoltaic array fault detection and diagnosis techniques," *International Journal of Photoenergy*, vol. 2019, Article ID 6953530, 19 pages, 2019.

[22] C. Li, "Comparative performance analysis of grid-connected PV power systems with different PV technologies in the hot summer and cold winter zone," *International Journal of Photoenergy*, vol. 2018, Article ID 8307563, 9 pages, 2018.

[23] D. D. Milosavljević, T. M. Pavlović, and D. S. Piršl, "Performance analysis of a grid-connected solar PV plant in Niš, republic of Serbia," *Renewable and Sustainable Energy Reviews*, vol. 44, pp. 423–435, 2015.

[24] P. M. Congedo, M. Malvoni, M. Mele, and M. G. De Giorgi, "Performance measurements of monocrystalline silicon PV modules in South-Eastern Italy," *Energy Conversion and Management*, vol. 68, pp. 1–10, 2013.

[25] D. Micheli, S. Alessandrini, R. Radu, and I. Casula, "Analysis of the outdoor performance and efficiency of two grid connected photovoltaic systems in northern Italy," *Energy Conversion and Management*, vol. 80, pp. 436–445, 2014.

[26] S. Edalati, M. Ameri, and M. Iranmanesh, "Comparative performance investigation of mono- and poly-crystalline silicon photovoltaic modules for use in grid-connected photovoltaic systems in dry climates," *Applied Energy*, vol. 160, pp. 255–265, 2015.

Hindawi
International Journal of Photoenergy
Volume 2022, Article ID 3852484, 13 pages
https://doi.org/10.1155/2022/3852484

Review Article

Imperative Role of Photovoltaic and Concentrating Solar Power Technologies towards Renewable Energy Generation

Vinod Kumar Sharma,[1] **Rajesh Singh**,[2] **Anita Gehlot**,[2] **Dharam Buddhi**,[2] **Simone Braccio**,[3] **Neeraj Priyadarshi**,[4] **and Baseem Khan**[5]

[1]*Department of Energy Technologies, Division of Bioenergy, Biorefinery and Green Chemistry, ENEA Research Centre Trisaia, 75026 Rotondella MT, Italy*
[2]*Division of Research & Innovation, Uttaranchal University, Uttarakhand, 248007, Dehradun, India*
[3]*Polytechnic of Bari, Italy*
[4]*CTiF Global Capsule, Dept. of Business Development and Technology, Aarhus University, Herning 7400, Denmark*
[5]*Department of Electrical and Computer Engineering, Hawassa University, Hawassa, Ethiopia 05*

Correspondence should be addressed to Baseem Khan; baseem.khan04@gmail.com

Received 2 December 2021; Revised 12 January 2022; Accepted 19 January 2022; Published 29 January 2022

Academic Editor: Amin Shahsavar

Copyright © 2022 Vinod Kumar Sharma et al. This is an open access article distributed under the Creative Commons Attribution License, which permits unrestricted use, distribution, and reproduction in any medium, provided the original work is properly cited.

The United Nations Development Programme (UNDP) 2030 agenda illustrates the requirement of expanding infrastructure and advancing technology for delivering modern and sustainable energy services for all in developing countries. Moreover, UNDP also set a goal of increasing the renewable energy share in the global energy. Renewable energy resources are eco-friendly and widely available resources from nature for generating energy. Geothermal energy, wind energy, solar energy, tidal energy, and biomass energy are renewable energy sources. Solar energy is one of the renewable energy generation approaches that harvests energy widely from sun radiation. Photovoltaic (PV) and concentrating solar power (CSP) are the primary technologies to capture solar energy. This study presents the significance of utilizing solar energy for electricity generation globally using PV and CSP technologies. Furthermore, the distinct energy capturing and storing mechanisms of PV and CSP technologies are presented in detail. This article presents the significance and implementation of thermal energy storage for storing energy obtained through CSP technology. Finally, the study presents a considerable gap between PV and CSP in terms of development with future trends.

1. Introduction

Over many years, momentum in establishing worldwide renewable energy sources has intensified. Renewable energies tend to be significant in the context of sustainable energy generation [1, 2], and the production of renewable resources worldwide, estimated at 20 percent, is primarily made up of biomass [3] and hydroelectricity [4]. The dramatic prospects for critical trends for the succeeding 60-70 years, assuming a "business as usual" behavior correlated with stable progress and demographic perspective for the southern and northern countries, embody profound transformation which is clearly shown in Figure 1.

Figures 2(a) and 2(b) present the statistical data regarding the anticipation rise in electricity demand. Moreover, the reduction of proven oil supplies, the prefoliation of nuclear plant safety like danger of nuclear waste accumulation, the spike of carbon dioxide concentration in the environment, etc. are the critical concerns of the next century (Figure 3). However, the fact remains that such innovations are not able to adapt to the need for increased power generation, environmental conservation, and a potential decline in the usage of coal and oil. As long as environmental pollution is related, renewable energy is crucial for reducing pollution in a sustainable manner [7, 8]. It has been anticipated that every billion kilowatt-hours of renewable energy will cut

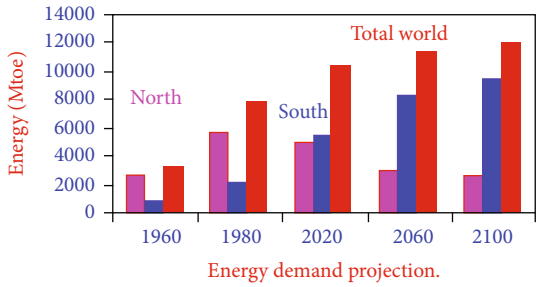

Figure 1: Energy demand projection (1960-2100) [5].

down sulfur emissions by 10,000 tonnes, particulate emissions by 2,000 tonnes, and carbon emissions by more than 200,000 tonnes [9]. There is an immediate need to build alternative energy sources that are environmentally sustainable. In spite of the above, it is of extreme significance that precise assessments are paid to appropriate measures such as a substantial reduction in energy use by the usage of alternative energy sources, energy conservation measures, and the combination of various types of energy. It should be pointed out that the reduction of energy demand is a daunting task, especially in terms of developing countries' needs, as it is intrinsically hard to operate in this field without an adverse effect on the development of the economy.

In 2017, ambient carbon dioxide levels were 406.5 parts per million, up 2.3 ppm relative to last year. The second hottest high was last year, just 0.99 Celsius in 2016, above the average of 1951-80 [11]. It is suggested that larger government supplies for clean energy sources would help to offset the more than 60 percent growth in world electricity demand over the midterm and quickly cross the coal divide in the United States, EU, China, India, and Mexico. A study [12] is carried out to optimize the heliostat layout in central receiver solar power plants in order to obtain optimum heliostat field efficiency using genetic algorithm, and the result concludes that increasing the tower height and decreasing the heliostat height by 7.7 and 19.5 percent, respectively, increase the total efficiency of the field by nearly 4% while decreasing the total area of heliostats by 17%. Innovative coolant tube layouts are developed and numerically modelled to achieve maximal exergy and energy efficiencies of photovoltaic-thermal (PV-T) systems [13]. Energy and exergy analyses of a photovoltaic-thermal system with wavy tubes are explored numerically using different coolant fluids to build a more efficient water-cooled photovoltaic-thermal system [14].

The contribution of the study is as follows:

(i) The overview and significance of solar energy are presented with statistics

(ii) The distinct types and mechanisms of photovoltaic (PV) and concentrated solar power (CSP) are presented

(iii) The implementation of thermal energy storage for storing the energy obtained through the CSP is addressed

(iv) A considerable gap between the PV and CSP technology is presented for future enhancement

The structure of the study is as follows: Section 2 covers the overview of solar energy and the importance of PV and CSP technologies for harvesting solar energy. Section 3 covers the concept of thermal energy storage for storing the energy obtained by CSP. Section 4 provides the considerable gap of development between PV and CSP, and the final section concludes the article.

2. Solar Energy

Solar power promises to be the primary technology for the transition to a decarbonized supply of energy among the numerous renewable energy sources, which can be installed almost throughout the world. The efficiency of the photovoltaic (PV) system is directly proportional to solar energy [15–17]. Many countries identify that renewables and energy conservation solutions are chosen to be a functional approach for combating coal usage. Solar resources are vast in Europe and worldwide, and a 98-gigawatt solar power plant is the highest power capacity built-in 2017 [18]. It is indeed worth remembering that, in 2017, a gross amount of USD 279.8 billion was apportioned to all renewables globally. The energy sector earned $2.5 billion on public markets in 2017, a spike of $1 billion in 2016 [19]. Across several energy scenarios, solar energy has been viewed as a critical factor.

The utilization of solar energy has split into two significant technologies based on solar radiation harvesting and transforming into electricity [20]. The technologies are solar photovoltaic (PV) and concentrated solar power (CSP) technology. The CSP enhances solar energy density and also provides both electricity and thermal power. On the other hand, PV is the only technology that provides flexibility or even lowers future costs; regardless of how fast the electricity prices are rising, in the future, solar power by both photovoltaic (PV) and concentrated solar power (CSP) seems to be a successful mechanism not only to fulfill the need for electricity in the globe but also to satisfy the demand for the depletion of fossil fuels from other sources. Meanwhile, numerous future clean energy systems are only photovoltaic technology that has a larger potential to prevent carbon emissions and tackle energy problems in the future [21]. "Power for World," an exciting initiative to encourage and provide electricity to more than a billion people in impoverished developed world countries, was initiated by Dr. Wolfgang Palz [22]. The industry has been abandoned because a photovoltaic plant with a total capacity of 10 GW is adequate to fulfill the minimum requirement of 10 Wp per person for the poorest inhabitants of the earth.

2.1. Photovoltaic (PV). As is the case today, PV is well accepted by most developed countries in the world. Several nations economically powerful sufficient, such as China, the United States, Japan, European countries, and India, have already made substantial investments in the growth of this specific field through their national programs [23].

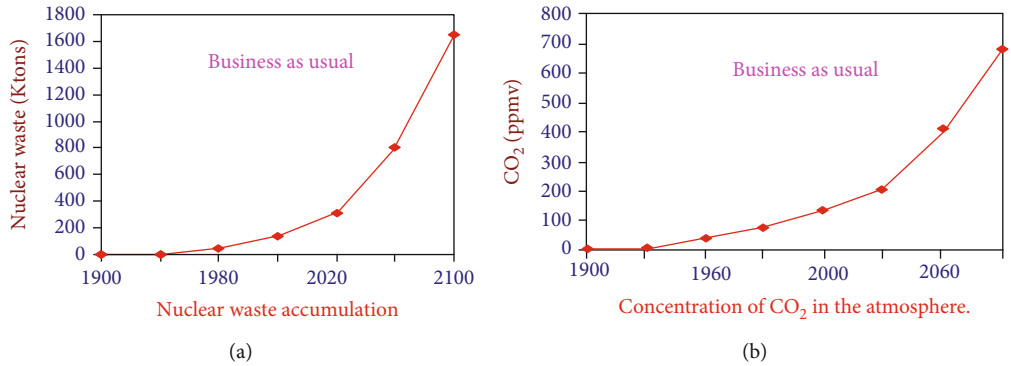

Figure 2: (a) Nuclear waste accumulation [6]. (b) Amount of CO_2 concentration level [6].

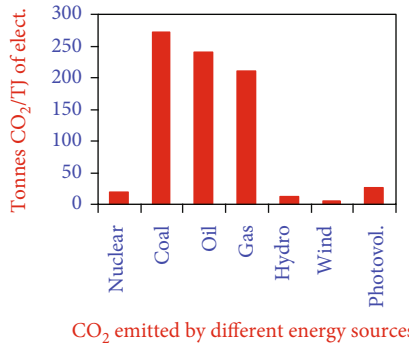

Figure 3: CO_2 emission from different energy sources [10]

The PV industry in the world has seen significant innovations. It is indeed noteworthy that photovoltaic, with built-in remote and central power stations generating hundreds of megawatts, is a technology that has already proven its reliability and is quite promising for the production of electrical energy on a global scale [24, 25]. The year 2019 was yet another streak year for the solar photovoltaic (PV) industry; about 60 GWp of new solar PV installations was installed throughout the year. Figure 4 demonstrates that by the end of the year, the global total deployed PV capacity is equivalent to 632.4 GW (gigawatt), and in 2019, the global cumulative solar capacity amounted to 633.7 GW and with 116.9 GW of new PV capacity installed in the same year [26]. Midterm projections for global combined PV capacity by 2020 increase from 600 GWp to 700 GWp, relying on the policy scenario. It is to be noted that the cumulative installed capacity of photovoltaic energy in 2019 in the European Union is mounted to be 134 GW. In contrast, it is expected that the same will be increasing to 370 GW in 2030 and up to 1051 GW in 2050.

In the foreseeable future, the European PV Technology and Innovation Platform (ETIP PV) benchmark scenario predicts that the global combined PV capacity will be about 9,000 GWp by 2050 [27]. Considering the International Energy Agency (IEA) demand growth scenario, this power will produce around one-third of the world's annual energy use, considering the International Energy Agency (IEA) demand growth scenario.

The main pillars of photovoltaics are divided into three categories: PV fabrication technologies, PV system technologies, and advanced services to industries [26], which are shown in Figure 5. Crystalline silicon-based (c-Si) modules currently have more than 90% market share and will be the predominant PV platform in the future [29]. In multijunction methods, the incorporation of layers of distinct materials to the roof of silicon might increasingly boost quality. The significant benefit of silicon-based PV modules is that the critical raw material, silicon, is the second most abundant (after oxygen) in the earth's crust [30]. Many PV cells are composed of silicon, refined, and filtered from silicon dioxide, which is sand. Very few thin-film products are available in the market, which is the amalgamation of copper indium gallium selenide (CIGS) and cadmium telluride (CdTe) [31].

However, thin-film technologies also weakened their comparative benefit over c-Si modules as silicon is now plentiful and very affordable which are illustrated in Figure 6(b). Thin films include rare elements such as indium and tellurium, which may be inconvenient if the production volumes were to escalate ten or a hundred times as anticipated by potential expansion [32]. Tellurium is almost as rare as platinum or copper, while silicon is about 60 million times more abundant than tellurium. First Solar is undoubtedly among the ten biggest PV module producers in the world, the only thin filmmaker [33]. Other PV technologies, such as organic or dye-sensitized cells, are also available but are still in the testing or demonstration process. They have a challenge with low efficiency and fast degradation in outdoor conditions, and it is not likely that they will ever be able to compete on a large scale with c-Si modules [34]. As of today, PV is well recognized by most of the industrialized countries in the world.

In 2015, solar energy attracted 56% of all new renewable energy investments or USD 161 billion [35]. Private sector interest in renewables is picking up but accelerating that interest will need a significant increase in concessional finance. The critical factor behind this accelerated growth is the drastic price decline of the solar PV modules. In nominal terms, the recent PV module price, 0.40-0.50 USD/Wp, is just 10 percent of the cost in 2008, and the price of the module will dip below $0.30/Wp, according to IHS Markit

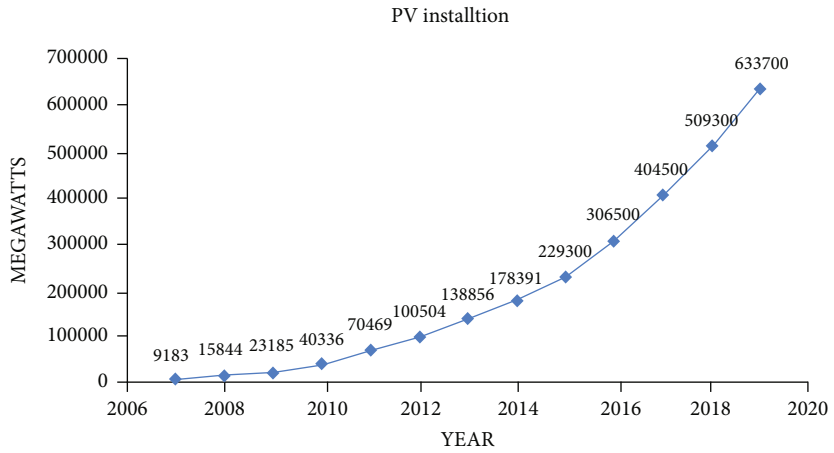

Figure 4: PV installations from 2000 to 2019 [28].

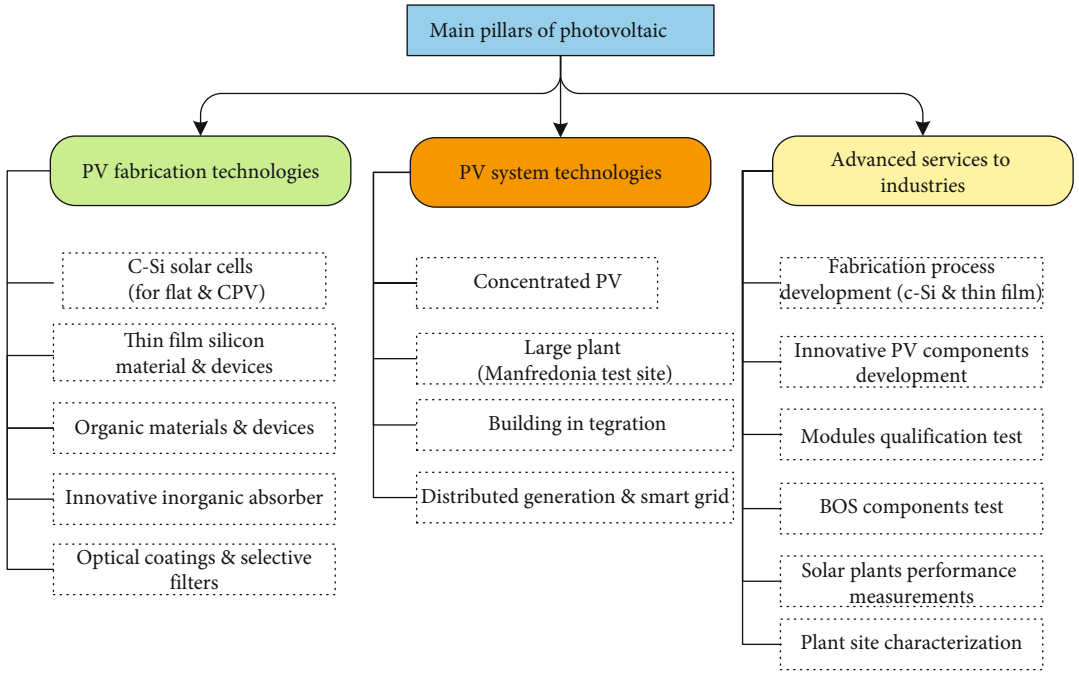

Figure 5: Main pillars of photovoltaics.

by 2020 [36]. ETIP PV will suggest a long-term basis scenario where the module's price is down to USD 0.10/Wp by 2050 [27].

In contrast to the modules, the PV system mounted contains components such as the Balance of System (BoS) inverters, wires, assembly, and construction structures. The contribution of the BoS cost in overall PV system capital (CAPEX) depends on the scale of the system. Still, typically less than half of it is utilized in large ground installations on competitive markets such as India [37]. The photovoltaic industry is effectively a semiconductor industry, where volume growth immediately reduces cost. The price of photovoltaic modules traditionally dropped by 20-25% each time the total installed capacity in the world doubled [38]. More effective use of materials, efficient processing methods, and enhanced efficiency of solar cells are the main determinants.

The average performance of PV modules is approximately around 16 percent and is expected to grow to 30 percent by 2050. Few commercial modules achieved 23 percent efficiency [39]. Best business modules now achieve a productivity of 23 percent. The automatic improvement in productivity lowers the PV CAPEX because about half the BoS cost is connected to the field. Better efficiency ensures that the PV modules use a smaller region every time. Best commercial modules already reach 23 percent efficiency which is shown in Figure 6. Increasing the efficiency drastically decreases the PV CAPEX because half of the BoS cost is area related. Better efficiency always means a smaller area required for the PV modules.

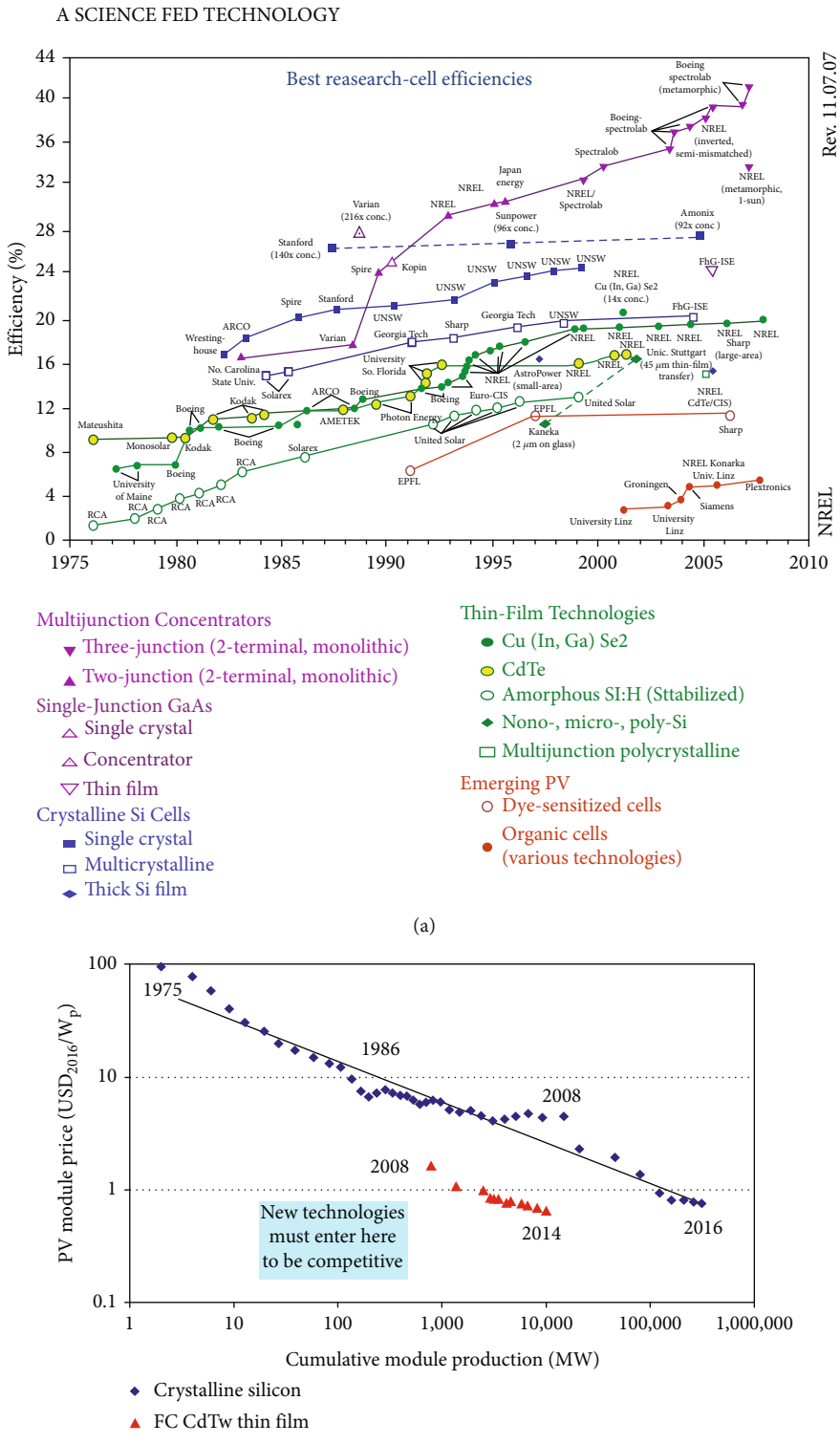

Figure 6: Continued.

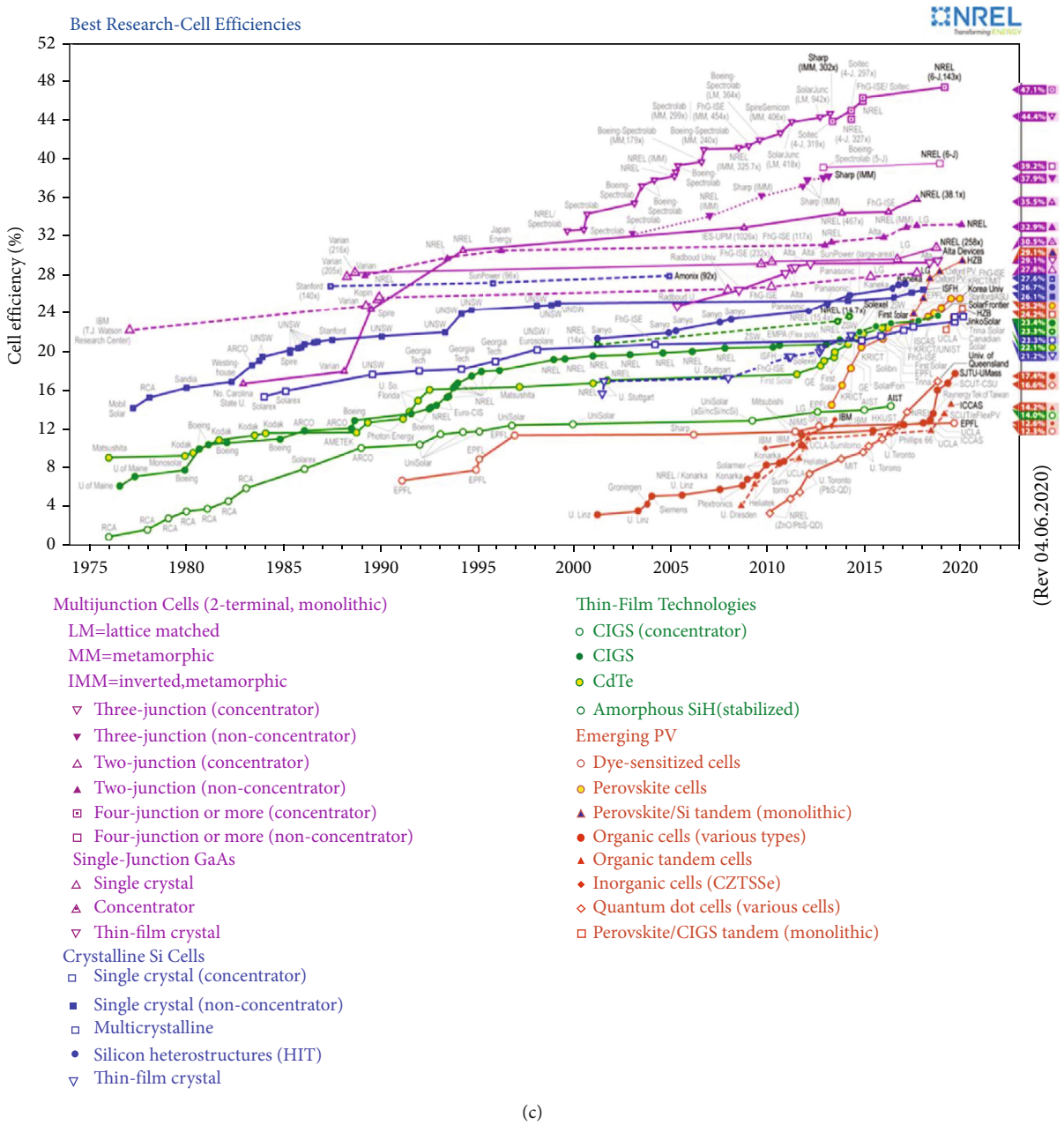

(c)

Figure 6: (a) The efficiency of materials. (b) Production and price relation. (c) The efficacy of cells [40].

In a climate zone, average temperatures have no significant effect on the output of solar panels. In fact, in more excellent conditions, solar panels are generally marginally more effective at generating electricity. If we reside in a cooler climate, you just get enough sunlight while the solar panels are working only a step farther north. Anyway, the terrific PV capacity growth was encouraged by reward mechanisms. According to the majority experts, grid parity can be attained before 2020 in most implementations and the early '20s in the remaining [41]. Complete form for consumer product (on-grid/off-grid) systems includes clocks, calculators, toys, greenhouse and production bunkers, residential applications, and electrical power plants. From 0.01 W up to 100 MW, residential applications are prevailing. Further drastic technical advances will lead to accurate market changes such as high-efficiency multilayers, quantum dots, and nanotubes and nanowires.

PV manufacturing is fundamentally a semiconductor industry, where the spike in production significantly reduces costs [42]. The average price of European crystalline silicon modules in 2017 dropped by 14% and is projected to fall by a further 15% in 2018 which has doubled; the pricing of PV modules has dropped 20-25 percent [43]. Other key factors are a more productive use of materials, more robust production practices, and better solar cell performance. Striking decrements in PV module cost is increasing BOS cost-share: from 30% to today's 50%. As for BOS cost decrement, perspectives are mainly linked to scale effects, but for

inverters (10% cost-share), average prices went down by 17% from 1990 to 2008, primarily due to efficiency increase (from 90% to 98%) [44]. Cutting down dangerous air pollution and diversifying energy supplies for a better source of safety may undoubtedly play a similar role, especially in the growth of low-carbon energy sources in emerging Asia as it was. Generation from renewables is expected to exceed 7600 TWh by 2021. Over the next five years, renewables will remain the fastest-growing source of electricity generation, with their share growing to 28% in 2021 from 23% in 2015 [45]. Notably, it makes an impressive remark that almost half a million solar panels were installed worldwide every day last year. Certainly, last year has been a turning point for renewables, but there is still proof that it continues on renewable growth for the transportation and for heat sectors to remain weak and in need of even stronger government efforts.

2.2. Concentrating Solar Power System (CSP). CSP is a mechanism of enhancing solar power density and delivering electricity and thermal power. Using different mirror configurations, CSP generates electric power by transforming the solar energy into high-temperature warmth; thereby, a typical generator is utilized for channeling the heat [46]. Plants contain two parts: one that harvests and transforms solar power into heat and the other that produces electricity from heating energy. CSP for the village is 10 km/w, and for the grid, applications may be scaled up to 100 megawatts [47]. During cloudy hours or at night, some devices have thermal storage available. Other elements can be paired with gas, and hybrid power stations will have dispatchable hybrid power. For thousands of years, CSP has been perceived and recognized by inventors. The origin of the current solar focus is believed to be in the seventeenth century. In the early 20th century, several new projects for concentrating varied from solar pumps to steam power turbines to distilling water. Concentrated solar (CS) technology is categorized into two distinct types, and they are shown in Figure 7. Tracking CS and nontracking are the two technologies of CSP.

There are four primary tracking CS technologies such as parabolic trough, solar tower, linear Fresnel reflectors, and parabolic dish defined based on the radius and technical treatment of the sun which are shown in Figure 8. Parabolic troughs are the most evolved CS methods and comprise most existing commercial plants. The parabola trough is the linear fixation collector composed of a cylindrically curved parabola mirror, reflecting the sunlight of a tube in the parabola focal line [48]. The tubular receiver comprises the heat-absorbing liquid and passes it into the furnace or other steam-making system through the circulation. The linear Fresnel reflector includes the FLR mirror tracking phase, which concentrates solar-based beam radiation onto a receiver tube mounted on the focal point of the Fresnel mirror and produces high-temperature working media to produce thermal cycle power [49]. Sunshine is converted into renewable energy by solar power towers. Many large heliostats are used to concentrate the sunlight on a receiver over a tower [50].

Parabolic-dish solar concentrators are two-axis solar tracking systems focusing solar radiation onto the heat receiver at the center point of the platform collector [52, 53]. The technical specifications of these four CS technologies are illustrated in Table 1. The capacity, implementation status, and operating year are discussed in the table. The parabolic dish Stirling tracking CS technology is installed in the outer environment, and it been operating from 1986 with a capacity of 10-25 kW.

3. Thermal Energy Storage

The attributable benefits of CSP innovations are achieved through the incorporation of traditional heat plants. A carbon burner is incorporated in conventional thermal cycles by thermal storage solar heat plants which can offer firm capabilities without needing to build separate backup power plants and without stochastic grid disturbance [55, 56]. Trough designs can incorporate thermal storage setting aside the heat transfer fluid in its hot phase allowing for electricity generation several hours into the evening [57]. All parabolic trough plants for this study are hybrids, meaning they use fossil fuel to supplement the solar output during periods of low solar radiation. Typically, a natural gas-fired heat or a gas steam boiler/preheater is used; troughs also can be integrated with existing coal-fired plants. The reflector follows the sun during the daylight hours by tracking along a single axis. A working fluid is heated to 150—350 oc as it flows through the receiver and then utilized as a heat source for a power generation system. The complete mechanism of the power generation is shown in Figure 9.

The Archimedes scheme integrates the best technologies of today with today's solar field, a storage facility, and a steam engine, the first of its kind in the world to be unveiled in Italy on 15 July 2010 [58]. Solar energy is stored in 360 linear parabolic collectors in the modular solar region. To optimize the working temperature and the capacity to store heat, the Italian National Agency for New Technologies, Energy and Sustainable Economic Development (ENEA), has unveiled a novel fluid heat carrier. The new concept of a concentrator based on thinner mirrors is another creative aspect of ENEA, saving building and installation expenses [59]. The utilization of ample heat storage enables the plant to heat the steam generator 24 hours a day at a uniform frequency regardless of the fluctuations in solar power availability. The steam generator includes heat exchangers "tube and shell" in which heat is transported to water to form superheated steam to be used in conventional thermoelectric plants. 5 MW solar plant worth almost €60 million has a specific characteristic to capture and store the solar thermal energy for several hours, allowing both off-sunshine and overcast sky power to be produced by the plant [60]. It is factual that the 2100 tonnes of oil saved and carbon dioxide emissions cut by 3250 tonnes over one year. The current findings represent a significant achievement, costing approximately five or six times more for the kilowatt-hour produced about the energy costs extracted using traditional fuels [10]. Access to large volumes of water is a significant obstacle for CSP use in arid areas because the water supplies

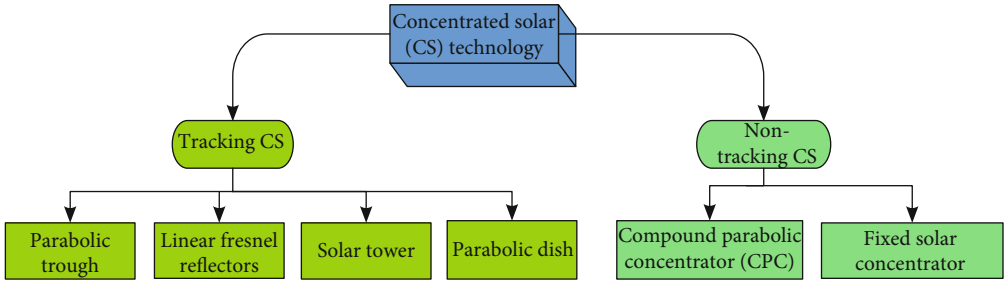

Figure 7: Concentrating solar technology.

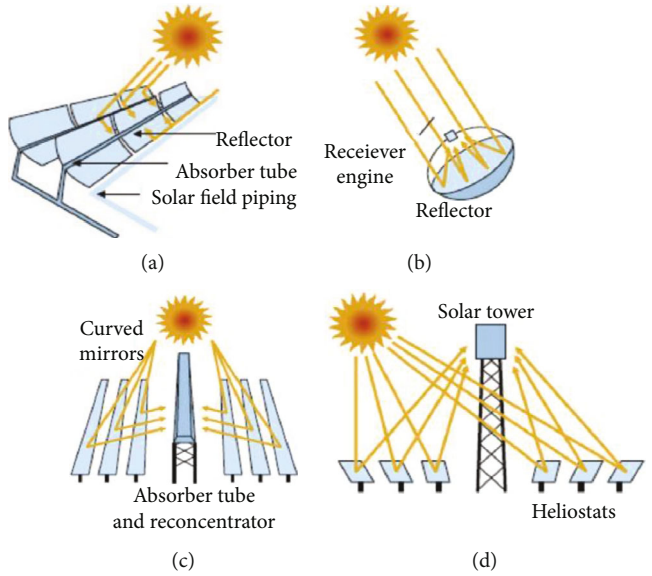

Figure 8: (a) Parabolic trough. (b) Dish Stirling. (c) Linear Fresnel reflectors. (d) Solar tower [51].

Table 1: Details of tracking CS [54].

Tracking CS	Capacity	Status	Operating
Parabolic trough	50-200 MW	Proven utility-scale technology	1984
Liner Fresnel reflectors	50-200 MW	In development	2012
Solar tower	50-100 MW	Demo plants built	2007
Parabolic dish Stirling	10-25 kW	Installation	1986

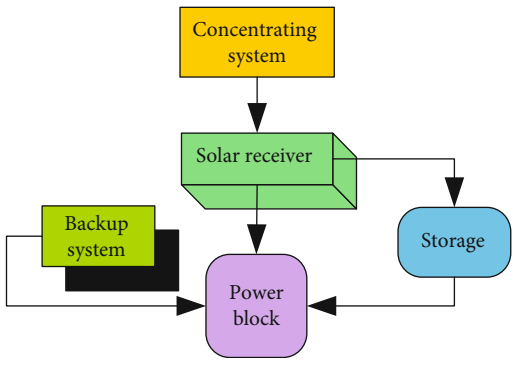

Figure 9: Process of thermal energy storage.

available are widely regarded by many stakeholders. Dry air cooling is a powerful alternative used in North Africa on the ISCC plants under development. However, it is more costly and reduces productivity. When installed in hot desert trough plants, it tends to decrease the annual production of energy by 7% and elevates the cost of electricity generated by approximately 10%. For solar towers, the efficiency penalty is less than for parabola dry cooling. Solar process heat promises an exciting future for the solar thermal industry, the need for industrial process heat is enormous, and many demonstration systems are fully operational. It is a technology ready for deployment and well-identified in the sector and the primary trend in research and development. Exceptionally, a medium-size solar process heating plant should be engineered, and feasibility analysis was undertaken out so

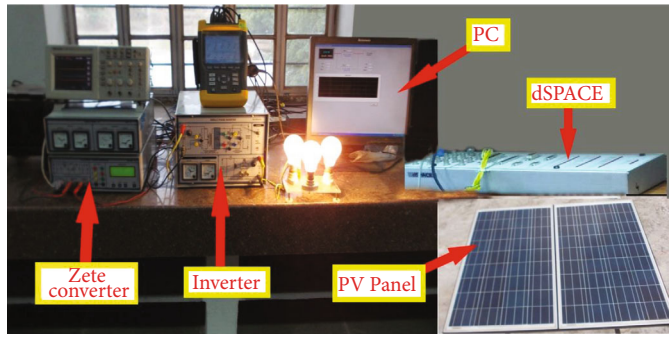

Figure 10: Hardware developed to set up in the laboratory.

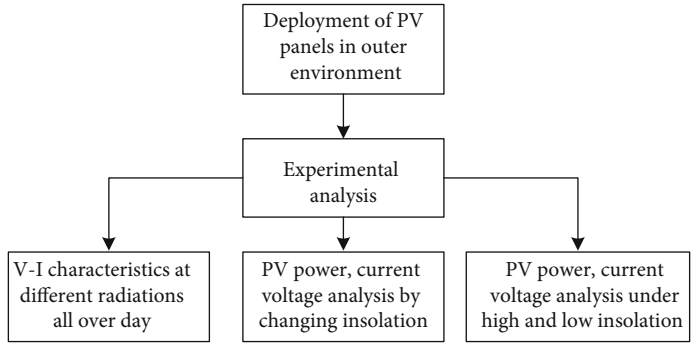

Figure 11: Flow chart of the proposed system.

that the graduates can realize the position of a system developer or an engineer in the industry.

4. Discussion

4.1. The Gap between PV and CSP Development. The CSP method operates only for irradiance, whereas the diffuse radiation can also be used for PV systems. The PV can then be mounted anywhere, while the required CSP areas are far more limited. PV plants will have opportunities for a dispersed and decentralized generation while CSP plants do not scale down well, and CSP production needs to provide a transmission grid. The photovoltaic system is primarily about solar panels, and CSP power plants incorporate a significant number of critical mechanical and chemical components. CSP plants require equal to 10 acres per MW, while crystalline technology needs around 4.5-5 acres of area for 1 MW of electricity, and thin-film technology requires about 6.5-7.5 hectares [61]. It is only an approximate criterion that can differ depending on panel technology and performance. In terms of materials, CSP plants demand a significant level of iron and cement. In contrast, in their manufacturing phase, PV plants need essential materials such as indium and rare earth elements.

In small-scale systems, the construction cost for photovoltaic plants is about 2,000-2,500 EUR/kW, and the price for the larger ones is just 1500 EUR/kW [62]. It is important to remember that, for both utility (MW-scale) and industrial (kW-scale) plants, the average cost of PV plants has been declining over the last few years, with a much less price decline to come in the future forecast. The infrastructure costs for CSP plants vary from 2,000-6,000 EUR/kW, depending on the technology, size, and potential usage of the heat storage facility. Ordinary annual operating costs for the photovoltaics plant are equivalent to 1% of initial expenditure compared with around 20/0 for CSR energy depletion. Moreover, the entire life span of the installation (ranging from 0.5 to 1% each year) has minor economic consequences for the CSP plant than for the PV plant. CSP generates more electricity than PV plants with the same rated capacity and the same environmental conditions. It demonstrates that the CSP's economic return is more substantial. PV systems are now the world's most common solar electric technologies.

At the end of 2015, over 235 GW of photovoltaic power systems had been installed worldwide, while there are now fewer than five GW of CSP technology [63]. Yet, this global CSP capacity is projected to reach up to 22 GW by 2025 with 1.2 GW of newly added capacity and a turnaround in activities shortly [64]. A few of the benefits of the CSP device are likely the conservation of heat. Power supply at peak time is an essential and demanding factor of power plant projects. As an intermediate phase to produce electricity over peak hours, CSP system provides the capacity to provide quick, reliable, and environmental storage of heat energy. Distinct technologies allow thermal storage for use in CSP systems. The second significant aspect is some possible technological transformations that might intensify CSP production in the area of "solar fuels." When comparing the CSP trend with the other sources of renewable energy, we can see that CSP

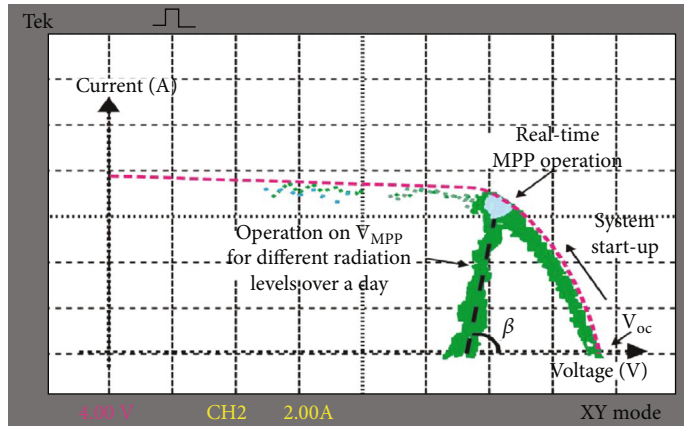

Figure 12: I-V characteristics under maximum power point condition.

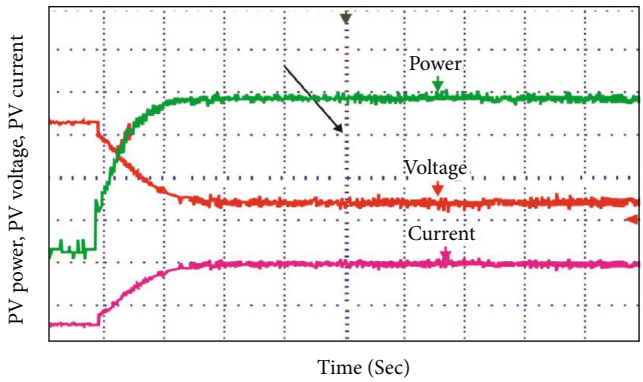

Figure 13: Practical obtained responses in changing solar insolation.

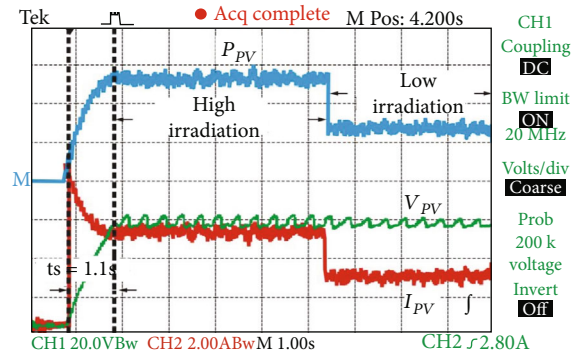

Figure 14: Practical results under high and low sun insolation conditions.

is at a significant shift. The initial and operational effect of CSP schemes would undoubtedly have a considerable impact on mirrors, vacuum receivers, optics, support systems, efficient heat transfer fluid, and turbines. CSP systems could provide about 10 percent of world energy in the most favorable circumstance [65]. The mass manufacturing of photovoltaic systems and public subsidies culminated in the development of low cost-effective multifunctional cells. In short, one technology cannot be claimed to be superior to another. Here, we tried to illustrate those problems that must be weighed before determining which solar energy is the best for a given situation.

Figure 10 illustrates an implementation of the PV system with dSPACE controller to check the power, voltage, and current characteristics under different irradiations. The flow chart of the proposed system is shown in Figure 11. The PV panel is deployed in the outer environment; the voltage obtaining from the PV is powered to the bulbs. The power to the bulb is provided by inverting the voltage obtaining from PV. The zeta converter can convert input voltage into a noninverted output voltage that might be lower or greater than the input voltage.

The system starts with maximum open-circuit voltage (V_{oc}) to account the real-time maximum power point operation (MPP) with varying I-V characteristics as represented by the pink dotted line (Figure 12). Further, the black dotted line represents the I-V characteristics of the solar cell operated at maximum power point voltage (V_{MPP}) for different radiation levels over a day. The variation in current with respect to voltage is demonstrated by an angle (β). Figure 13 describes the actual functioning of the solar cell (respective to power, voltage, and current parameters) upon irradiation. It is visible that with increasing irradiation time, the voltage across the cell decreases with increasing current and further becomes constant confirming the accurate behavior of the solar system.

The practical current responses of the proposed PV system under low and high sun insolation have been realized at obtained constant voltage as shown in Figure 14. It is observed that the exhibited current is higher at high irradiation compared to low irradiation. Hence, higher power is gained at high irradiation. Payback analysis, net benefit analysis, saving-to-investment ratio, adjusted internal rate of return, and life-cycle cost analysis are five economic analysis parameters that are frequently used for solar PV plant placement. Currently, in this study, the proposed system is shown as proof of concept for showing significance of the PV system for electricity generation. In the future, the proposed system will be deployed in a wide range and the economic aspects of the system will be evaluated in detail.

5. Conclusion

The UNDP set a target of comprehensive implementation of renewable energy sources for minimizing the impact of carbon emissions on the environment. Renewable energy sources have the potential to generate sustainable electricity for all. Solar energy is one of the prominent renewable energies that is generated through the radiation of the sun. At present, solar energy is widely implemented in many countries to meet the electricity demand sustainably. PV and CSP are the two different technologies utilized to capture the heat generated from the sun. This article presents the mechanism, types, and advancement of PV and CSP technology concerning the widely implemented technologies in many countries for electricity generation. Thermal energy storage is one of the prominent technologies utilized for storing the heat energy obtained through CSP. A gap between the PV and CSP technologies is presented in the article to enhance the performance. As part of the proof of concept, an experiment is carried with PV panels in the outer environment. The power, current, and voltage analysis of the suggested system are evaluated in this experiment, and it is found that the observed current is higher at high irradiation relative to low irradiation. In the future scope, PV and CSP technologies play a crucial role for the generation of renewable power in a sustainable manner that minimizes impact on the environment.

Data Availability

Data will be available on request. For the data-related queries, kindly contact Vinod Kumar Sharma (vinodkumar.swarma@enea.it).

Conflicts of Interest

The authors declare that they have no conflicts of interest.

References

[1] A. Nandi and V. K. Kamboj, "A new solution to profit based unit commitment problem considering PEVs/BEVs and renewable energy sources," in *E3S Web of Conferences*, p. 8, Punjab, India, 2020.

[2] P. Verma, H. Bedi, and R. K. Sharma, *Integrated utilization of solar energy in a zero energy building (ZEB): an approach towards sustainable development*, International Science Press, Phagwara, India, 2016.

[3] A. Churasia, J. Singh, and A. Kumar, "Production of biodiesel from soybean oil biomass as renewable energy source," *Journal of Environmental Biology*, vol. 37, no. 6, pp. 1303–1307, 2016.

[4] P. A. Owusu and S. Asumadu-Sarkodie, "A review of renewable energy sources, sustainability issues and climate change mitigation," *Cogent Engineering*, vol. 3, no. 1, article 1167990, 2016.

[5] "Energy projections, calculating long term energy demand |IAEA," November 2021, https://www.iaea.org/topics/energy-projections.

[6] Z. Hausfather and J. Ritchie, "A 3C world is now 'business as usual, The Breakthrough Institute," November 2021, https://thebreakthrough.org/issues/energy/3c-world.

[7] V. Suresh, S. Sreejith, S. K. Sudabattula, and V. K. Kamboj, "Demand response-integrated economic dispatch incorporating renewable energy sources using ameliorated dragonfly algorithm," *Electrical Engineering*, vol. 101, no. 2, pp. 421–442, 2019.

[8] M. Sharma, J. Singh, C. Baskar, and A. Kumar, "A comprehensive review of renewable energy production from biomass-derived bio-oil," *BioTechnologia. Journal of Biotechnology Computational Biology and Bionanotechnology*, vol. 100, no. 2, pp. 179–194, 2019.

[9] M. L. Mittal, "Estimates of emissions from coal fired thermal power plants in India," in *2012 International emission inventory conference*, pp. 1–22, New Delhi India, 2010.

[10] L. Abdallah and T. El-Shennawy, "Reducing carbon dioxide emissions from electricity sector using smart electric grid applications," *Journal of Engineering*, vol. 2013, Article ID 845051, 8 pages, 2013.

[11] "Climate change indicators: atmospheric concentrations of greenhouse gases, Climate Change Indicators in the United States, US EPA," December 2021, https://www.epa.gov/climate-indicators/climate-change-indicators-atmospheric-concentrations-greenhouse-gases.

[12] P. Talebizadeh, M. A. Mehrabian, and H. Rahimzadeh, "Optimization of heliostat layout in central receiver solar power plants," *Journal of Energy Engineering*, vol. 140, no. 4, article 4014005, 2014.

[13] A. H. Eisapour, M. Eisapour, M. J. Hosseini, A. H. Shafaghat, P. Talebizadeh Sardari, and A. A. Ranjbar, "Toward a highly efficient photovoltaic thermal module: energy and exergy analysis," *Renewable Energy*, vol. 169, pp. 1351–1372, 2021.

[14] M. Eisapour, A. H. Eisapour, M. J. Hosseini, and P. Talebizadehsardari, "Exergy and energy analysis of wavy tubes photovoltaic-thermal systems using microencapsulated PCM nano-slurry coolant fluid," *Applied Energy*, vol. 266, article 114849, 2020.

[15] R. Singh, S. Kumar, A. Gehlot, and R. Pachauri, "An imperative role of sun trackers in photovoltaic technology: a review," *Renewable and Sustainable Energy Reviews*, vol. 82, pp. 3263–3278, 2018.

[16] D. Dhawale and V. K. Kamboj, "Scope of intelligence approcahes for unit commitment under uncertain sustainable energy environment for effective vehicle to grid operations-a comprehensive review," in *E3S Web of Conferences*, p. 1034, India, 2020.

[17] O. Bamisile, S. Obiora, Q. Huang et al., "Towards a sustainable and cleaner environment in China: dynamic analysis of vehicle-to-grid, batteries and hydro storage for optimal RE integration," *Sustainable Energy Technologies and Assessments*, vol. 42, article 100872, 2020.

[18] "The biggest solar power plants in the world," https://www.power-technology.com/features/the-worlds-biggest-solar-power-plants/.

[19] "World Energy Outlook 2017 analysis - IEA," https://www.iea.org/reports/world-energy-outlook-2017.

[20] X. Ju, C. Xu, Y. Hu, X. Han, G. Wei, and X. Du, "A review on the development of photovoltaic/concentrated solar power (PV-CSP) hybrid systems," *Solar Energy Materials & Solar Cells*, vol. 161, pp. 305–327, 2017.

[21] D. Gielen, F. Boshell, D. Saygin, M. D. Bazilian, N. Wagner, and R. Gorini, "The role of renewable energy in the global energy transformation," *Energy Strategy Reviews*, vol. 24, pp. 38–50, 2019.

[22] W. Palz, "*Power for the world: the emergence of electricity from the Sun*," Pan Stanford Publishing, 2021, https://www.routledge.com/Power-for-the-World-The-Emergence-of-Electricity-from-the-Sun/Palz/p/book/9789814303378.

[23] J. C. R. Kumar and M. A. Majid, "Renewable energy for sustainable development in India: current statusfuture prospects challenges employment and investment opportunities," *Energy Sustainability and Society*, vol. 10, no. 1, pp. 1–36, 2020.

[24] M. Sharma, K. Bansal, and D. Buddhi, "Real time data acquisition system for performance analysis of modified PV module and derivation of cooling coefficients of electrical parameters," *Procedia Computer Science*, vol. 48, pp. 582–588, 2015.

[25] M. Sharma, K. Bansal, and D. Buddhi, "Operating temperature of PV module modified with surface cooling unit in real time condition," in *2014 IEEE 6th India International Conference on Power Electronics (IICPE)*, Kurukshetra, India, 2015.

[26] "Global new installed solar PV capacity 2019 Statista," https://www.statista.com/statistics/280200/global-new-installed-solar-pv-capacity/.

[27] "LCOE & competitiveness - ETIP PV.," https://etip-pv.eu/about/working-groups/lcoe-competiveness/.

[28] *Market Report Series: Renewables 2017 analysis - IEA*https://www.iea.org/reports/renewables-2017.

[29] T. S. Ustun, Y. Nakamura, J. Hashimoto, and K. Otani, "Performance analysis of PV panels based on different technologies after two years of outdoor exposure in Fukushima, Japan," *Renewable Energy*, vol. 136, pp. 159–178, 2019.

[30] X. Su, Q. Wu, J. Li et al., "Silicon-based nanomaterials for lithium-ion batteries: a review," *Advanced Energy Materials*, vol. 4, no. 1, article 1300882, 2014.

[31] J. Ramanujam and U. P. Singh, "Copper indium gallium selenide based solar cells - a review," *Energy and Environmental Science*, vol. 10, no. 6, pp. 1306–1319, 2017.

[32] T. D. Lee and A. U. Ebong, "A review of thin film solar cell technologies and challenges," *Renewable and Sustainable Energy Reviews*, vol. 70, pp. 1286–1297, 2017.

[33] N. Kannan and D. Vakeesan, "Solar energy for future world: - a review," *Renewable and Sustainable Energy Reviews*, vol. 62, pp. 1092–1105, 2016.

[34] S. Almosni, A. Delamarre, Z. Jehl et al., "Material challenges for solar cells in the twenty-first century: directions in emerging technologies," *Science and Technology of Advanced Materials*, vol. 19, no. 1, pp. 336–369, 2018.

[35] O. Chernyak, Y. Chernyak, and Y. Fareniuk, "Forecasting of global new investment in renewable energy," *HAICTA*, vol. 2030, pp. 272–278, 2017.

[36] "Solar PV module manufacturing base continues to consolidate in 2020 IHS Markit," https://ihsmarkit.com/research-analysis/solar-pv-module-manufacturing-base-continues-consolidate-2020.html.

[37] E. Vartiainen, G. Masson, C. Breyer, D. Moser, and E. Román Medina, "Impact of weighted average cost of capital capital expenditure and other parameters on future utility-scale PV levelised cost of electricity," *Progress in Photovoltaics: Research and Applications*, vol. 28, no. 6, pp. 439–453, 2020.

[38] "Solar photovoltaic electricity solar generation 6 solar photovoltaic electricity," *European Photovoltaic Industry Association—EPIA*, 2011.

[39] E. Hannah, M. Duncan, and G. T. André, "Renewables 2019 Global Status Report," December 2021, https://www.ren21.net/gsr-2019/.

[40] A. Blakers, N. Zin, K. R. Mcintosh, and K. Fong, "High efficiency silicon solar cells," *Energy Procedia*, vol. 33, pp. 1–10, 2013.

[41] G. Persen, *How do the EU's climate and energy policies affect Norwegian electricity prices and the outlook for profitable wind power development in 2030? [M.S. thesis]*, Norwegian School of Economics, Supervisor Linda Nøstbakken, Bergen, Spring, 2017.

[42] "(18) Semiconductor industry steps into the solar PV market Request PDF," https://www.researchgate.net/publication/297781288_Semiconductor_industry_steps_into_the_solar_PV_market.

[43] M. Woodhouse, B. Smith, A. Ramdas, and R. Margolis, *Crystalline silicon photovoltaic module manufacturing costs and sustainable pricing: 1H 2018 benchmark and cost reduction roadmap*, National Renewable Energy Lab.(NREL), Golden, CO (United States), 2019.

[44] M. GREEN, "Solar cell efficiency tables (version 40)," *IEEE Transactions on Fuzzy Systems*, vol. 20, no. 6, pp. 1114–1129, 2012.

[45] "IEA raises its five-year renewable growth forecast as 2015 marks record year - news – IEA," https://www.iea.org/news/iea-raises-its-five-year-renewable-growth-forecast-as-2015-marks-record-year.

[46] M. Mehos, *Concentrating Solar Power Gen3 Demonstration Roadmap*, Golden, CO (United States), 2017.

[47] "Concentrating Solar Power Technology: Principles, Developments and Applications - Google Books," https://books.google.co.in/books?hl=en&lr=&id=V6NgAgAAQBAJ&oi=fnd&pg=PP1&dq=concentrating+solar+power+technology&ots=nugR3aP40D&sig=ilWdCW7PHRmB7Z1uZeu4oehf3Os#v=onepage&q=concentrating solar power technology&f=false..

[48] G. K. Manikandan, S. Iniyan, and R. Goic, "Enhancing the optical and thermal efficiency of a parabolic trough collector – a review," *Applied Energy*, vol. 235, pp. 1524–1540, 2019.

[49] M. Alhaj, A. Mabrouk, and S. G. Al-Ghamdi, "Energy efficient multi-effect distillation powered by a solar linear Fresnel collector," *Energy Conversion and Management*, vol. 171, pp. 576–586, 2018.

[50] R. Chen, Z. Rao, and S. Liao, "Determination of key parameters for sizing the heliostat field and thermal energy storage in solar tower power plants," *Energy Conversion and Management*, vol. 177, pp. 385–394, 2018.

[51] Y. Zhao, A. Dunn, J. Lin, and D. Shi, *Photothermal Effect of Nanomaterials for Efficient Energy Applications*, Elsevier Inc., 2018.

[52] R. D. Jilte, J. K. Nayak, and S. B. Kedare, "Experimental investigation on heat losses from differentially heated cylindrical cavity receiver used in paraboloid concentrator," *Journal of Solar Energy Engineering*, vol. 139, no. 3, 2017.

[53] L. G. Pheng, R. Affandi, M. R. Ab Ghani, G. C. Kim, and Z. Zano, "Study the feasibility of Parabolic Dish (PD) from several prospective criteria in Malaysia environment," *Journal of Engineering and Applied Science*, vol. 11, no. 6, pp. 3929–3937, 2016.

[54] H. L. Zhang, J. Baeyens, J. Degrève, and G. Cacères, "Concentrated solar power plants : review and design methodology," *Renewable and sustainable energy reviews*, vol. 22, pp. 466–481, 2013.

[55] D. Wendt, H. Huang, G. Zhu et al., "Geologic thermal energy storage of solar heat to provide a source of dispatchable renewable power and seasonal energy storage capacity," *GRC Transactions*, vol. 43, pp. 73–91, 2019.

[56] D. Buddhi, R. Kumar, and R. Singh, "Thermal energy management in textile industries," vol. 5, no. 4, pp. 438–450, 2018.

[57] A. Häberle, *Concentrating solar technologies for industrial process heat and cooling In Concentrating Solar Power Technology*, Woodhead Publishing, 2012.

[58] A. Maccari, D. Bissi, G. Casubolo et al., "Archimede solar energy molten salt parabolic trough demo plant: a step ahead towards the new frontiers of CSP," *Energy Procedia*, vol. 69, pp. 1643–1651, 2015.

[59] A. Castaldo, G. Vitiello, E. Gambale, M. Lanchi, M. Ferrara, and M. Zinzi, "Mirroring solar radiation emitting heat toward the universe: design, production, and preliminary testing of a metamaterial based daytime passive radiative cooler," *Energies*, vol. 13, no. 16, p. 4192, 2020.

[60] J. J. C. S. Santos, J. C. E. Palacio, A. M. M. Reyes, M. Carvalho, A. J. R. Freire, and M. A. Barone, "Concentrating solar power," *Adv. Renew. Energies Power Technol.*, vol. 1, no. 2, pp. 373–402, 2018.

[61] "How much land is required for solar PV farms," http://www.solarmango.com/ask/2015/10/09/how-much-land-is-required-for-solar-pv-farms/.

[62] "JRC Science for Policy Report, 2019," November 2021, https://ec.europa.eu/jrc/sites/default/files/pesetaiv_summary_final_report.pdf.

[63] K. Mohammadi and H. Khorasanizadeh, "The potential and deployment viability of concentrated solar power (CSP) in Iran," *Energy Strategy Reviews*, vol. 24, pp. 358–369, 2019.

[64] A. K. Singh and A. H. Idrisi, "Evolution of renewable energy in India: wind and solar," *Journal of The Institution of Engineers (India): Series C*, vol. 101, no. 2, pp. 415–427, 2020.

[65] A. Bielecki, S. Ernst, W. Skrodzka, and I. Wojnicki, "Concentrated solar power plants with molten salt storage: economic aspects and perspectives in the European Union," *International Journal of Photoenergy*, vol. 2019, Article ID 8796814, 10 pages, 2019.